Recent Advances in Research and Forecasting of Tropical Cyclone Track, Intensity, and Structure at Landfall

Marie-Dominique Leroux, Russel L. Elsberry, Esperanza O. Cayanan, Eric Hendricks, Matthew Kucas, Peter Otto, Robert Rogers, Buck Sampson, Zifeng Yu, Kimberly Wood

RECENT ADVANCES IN RESEARCH AND FORECASTING OF TROPICAL CYCLONE TRACK, INTENSITY, AND STRUCTURE AT LANDFALL

Marie-Dominique Leroux
Météo-France DIROI/EC, La Réunion, France

Kimberly Wood
Mississippi State University, Mississippi State, USA

Russell L. Elsberry
University of Colorado-Colorado Springs, Colorado Springs, USA

Esperanza O. Cayanan
Philippine Atmospheric, Geophysical and Astronomical Services Administration, Metro Manila, Philippines

Eric Hendricks
Naval Postgraduate School, Monterey, USA

Matthew Kucas
Joint Typhoon Warning Center, Hawaii, USA

Peter Otto
Bureau of Meteorology, Melbourne, Australia

Robert Rogers
NOAA/AOML/Hurricane Research Division, Miami, USA

Buck Sampson
Naval Research Laboratory, Monterey, USA

Zifeng Yu
Shanghai Typhoon Institute and Laboratory of Typhoon Forecast Technique, China Meteorological Administration, Shanghai, China

ABSTRACT

This review prepared for the fourth International Workshop on Tropical Cyclone Landfall Processes (IWTCLP-4) summarizes the most recent (2015-2017) theoretical and practical knowledge in the field of tropical cyclone (TC) track, intensity, and structure rapid changes at or near landfall. Although the focus of IWTCLP-IV was on landfall, this summary necessarily embraces the characteristics of storms during their course over the ocean prior to and leading up to landfall. In the past few years, extremely valuable observational datasets have been collected for TC forecasting guidance and research studies using both aircraft reconnaissance and new geostationary or low-earth orbiting satellites at high temporal and spatial resolution. Track deflections for systems near complex topography such as that of Taiwan and La Réunion have been further investigated, and advanced numerical models with high spatial resolution necessary to predict the interaction of the TC circulation with steep island topography have been developed. An analog technique has been designed to meet the need for longer range landfall intensity forecast guidance that will provide more time for emergency preparedness. Probabilistic track and intensity forecasts have also been developed to better communicate on forecast uncer-

Corresponding author: Marie-Dominique Leroux, mariedominique.leroux@gmail.com

DOI: 10.6057/2018TCRR02.02

tainty. Operational practices of several TC forecast centers are described herein and some challenges regarding forecasts and warnings for TCs making landfall are identified. This review concludes with insights from both researchers and forecasters regarding future directions to improve predictions of TC track, intensity, and structure at landfall.

Keywords: tropical cyclone, track, intensity, structure, landfall, rapid intensification, rapid changes

1. Introduction

Hazards associated with tropical cyclone (TC) landfall pose increasing risks as coastal populations grow, yet accurate forecasts of the timing, location, and impacts of TC landfall remain an ongoing challenge. In October 2017, Typhoon Hato made landfall in South China near Macau after rapidly intensifying (http://www.hko.gov.hk/informtc/hato17/hato.htm) as defined by a minimum increase of 15.4 m s^{-1} day^{-1} in the maximum surface wind speed. Strong winds and flooding affected most of Macau, and Hato's storm surge caused record-high sea levels. Estimated economic losses from Hato were about USD $4.3 billion in China and at least USD $1.4 billion in Macau, and 27 fatalities have been reported.

Queensland, Australia, was impacted by two strong TCs in recent years, Cyclone Marcia (2015) and Cyclone Debbie (2017). Both TCs rapidly intensified the bay before landfall. After Marcia made a sharp turn, its strong winds devastated portions of the coastline and damaged numerous structures (http://www.bom.gov.au/cyclone/history/marcia.shtml). In addition to damage along the coast, Debbie caused extensive inland flooding during the days after landfall. Overall, Debbie's impacts resulted in an estimated USD $1.8 billion in damage and 14 fatalities (Podlaha et al. 2017).

These recent cases demonstrate the ongoing need to improve our understanding and prediction of rapid changes in TC track, intensity, and structure near landfall, which relies on a proper characterization of the near-coastal atmospheric environment. Structural changes near and during landfall subsequently affect the distribution of hazardous winds and heavy rainfall, and since that rain may extend far inland, these structural changes impact the potential for flooding.

Similar to the previous IWTCLP-3 report by Cheung (2014), this report summarizes recent (past three years) advances in research on rapid changes in TC track, intensity, and structure both near landfall and over the open ocean. It also describes operational practices and challenges regarding forecasts and warnings of these systems as they approach land. The report concludes with recommended routes for research and operations to improve TC track, intensity, and structure prediction at and near landfall. The paper contains six sections aside from the introduction and conclusion; they are represented by the five main branches of the comprehensive map given at the end of the manuscript. Online documentation, including working documents, reports, and presentations for the IWTCLP-IV can be found at the WMO site, http://www.wmo.int/pages/prog/arep/wwrp/new/IWTCLP4-ppt.html.

2. Recent advances in TC observing systems

Accurate analysis of TC position, intensity, and structure are particularly crucial for TCs making landfall, especially when these variables are rapidly changing. While geostationary satellites are the primary data source for TC position, scatterometer and microwave sensor imagery from low-earth orbiting (LEO) satellites provide essential information on convective structure and thus rainfall distribution.

The next-generation Advanced Baseline Imager (ABI; Schmit et al. 2017) is now operational on the National Oceanic and Atmospheric Administration (NOAA) Geostationary Operational Environmental Satellite (GOES-16), providing 15-minute full disk imagery in 16 bands. The geostationary Himawari-8 satellite, operated by the Japan Meteorological Agency (JMA), has a similar instrument with 16 bands that can produce 10-minute full disk imagery. Since Himawari-8 became operational in 2015, its frequent observations have improved forecasters' ability to monitor and track TCs in the western Pacific Ocean. Although the GOES-16 ABI was not officially operational during the 2017 North Atlantic hurricane season, its preliminary observations provided additional, invaluable information to forecasters, and researchers will utilize these data to improve numerical model guidance products. For example, numerical models shall benefit from the assimilation of atmospheric motion vectors and land and sea surface temperatures, while cloud products and estimated rainfall rates may be used to verify model output (Schmit et al. 2017).

Unfortunately, not all TC basins have next-generation satellite observations to improve warnings and risk mitigation strategies. The southwest Indian Ocean (SWIO) has comparatively limited satellite coverage despite the vulnerable populations at risk from TC landfall. Madagascar, which is the fourth largest island on earth and one of the poorest countries in the world, was directly hit twice a year by TCs during the 1999/2000 to 2015/16 seasons - one third of these TCs making landfall at the hurricane strength stage (Leroux et al. 2018). Mozambique, another poor country on the east coast of Africa between Tanzania and South Africa, was hit once a year by TCs and about once every three years by TCs of hurricane strength, on average. Note that Meteosoat-8, the first satellite of the Meteosat second generation series was moved in 2017 over the SWIO and

offers better resolution images and more channels than the older Meteosat 7 satellite.

Two recently launched polar-orbiting satellites, the European Space Agency (ESA) Soil Moisture and Ocean Salinity (SMOS) mission and the National Aeronautics and Space Administration (NASA) Soil Moisture Active Passive (SMAP) mission, can provide TC observations in data-void areas such as the SWIO. Both SMAP and SMOS carry microwave radiometers with L-band frequency (~1.4GHz) and wavelengths of ~21 cm. Such long wavelengths are largely unaffected by precipitation and can thus observe TC inner cores. The passes can be infrequent (~ 3 days) and real-time access is still a challenge, yet these sensors provide a unique data set given their wide swath (~1000 km) and ability to estimate inner core wind speeds (Meissner et al. 2017; Reul et al. 2017).

In addition, microsatellites can provide TC inner-core observations on restricted budgets. On 15 December 2016, NASA deployed the Cyclone Global Navigation Satellite System (CYGNSS) to observe the globe between 38°S and 38°N. The primary objectives of CYGNSS are to measure the ocean surface wind speed (but not direction) in the TC inner core from formation through rapid intensification to decay and extratropical transition. The eight CYGNSS spacecraft receive Global Positioning System (GPS) signals reflected from the earth's surface, resulting in 32 surface wind measurements per second. Like SMAP and SMOS, GPS signals are at a long (L-band) wavelength unaffected by precipitation, thus surface wind speed estimates can theoretically be obtained in the TC eyewall region (e.g., Morris and Ruf, 2017). Efforts are underway to collect observations from reconnaissance and research aircraft during CYGNSS overflights to verify CYGNSS measurements.

The greatest limitation of the CYGNSS mission is that only eight spacecraft are in orbit. While the 90-minute swath coverage may be adequate for a TC at 30°N, the longitudinal spacing between the eight spacecraft grows progressively larger toward the equator and thus increases the chance of CYGNSS not observing a TC's complete structure (Fig. 1). The median revisit time is around 3 hours while the mean revisit time is around 7 hours. Also, the CYGNSS surface wind measurements are not presently collected in real time due to logistical limitations. The CYGNSS constellation was launched as a research program and more ground stations or more frequent data downloads are required for real-time collection. However, if the limitations on the numbers of spacecraft, ground-station availability, and data download costs and capacity can be overcome, forecasters and researchers will have a new source of TC intensity and structure observations with two-dimensional analyses of surface wind speeds, including within the TC inner core.

In addition to satellite-based observing systems, the NOAA Hurricane Research Division (HRD) continues to collect extremely valuable observational datasets [mainly in the North Atlantic (NATL) basin but also in the eastern North Pacific (EPAC)] for TC research and in support of National Hurricane Center (NHC) operational forecasts. These NOAA aircraft missions focus on collecting observations to improve the understanding and prediction of TC intensity change under the NOAA Intensity Forecasting Experiment (IFEX; Rogers et al. 2013). During 2015, HRD collaborated with the U. S. Office of Naval Research's Tropical Cyclone Intensity (TCI-15) field experiment to observe Hurricane Patricia (2015), the most intense hurricane on record in the EPAC (Rogers et al. 2017). Doyle et al. (2017) describes the special observations collected in TCI-15, including the High Density Sounding System (HDSS) dropwindsondes deployed from the U.S. NASA WB-57 aircraft flying at 60,000 ft. Recently, HRD successfully collected extensive aircraft datasets during the rapid intensification of Hurricane Harvey (2017) prior to landfall

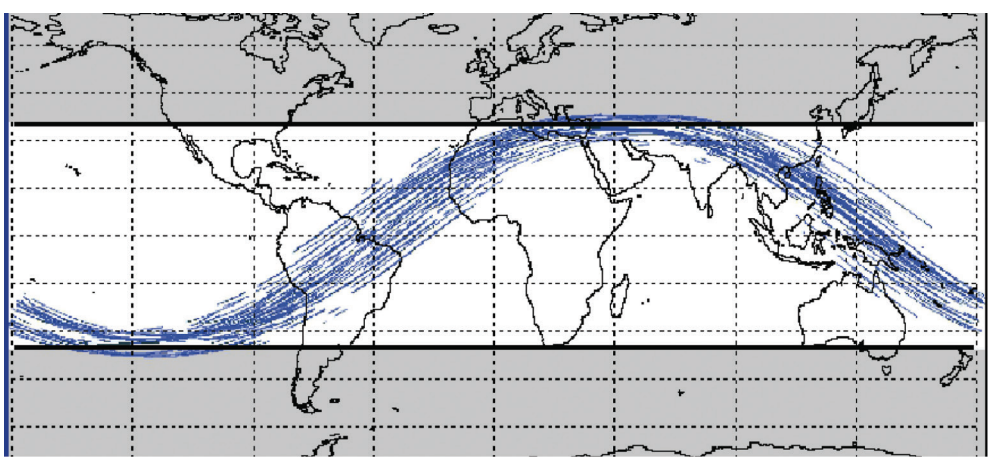

Fig. 1. 90-minute coverage of the eight CYGNSS spacecraft, which are positioned in low earth orbit at an inclination of 35°.

in Texas and as Hurricane Irma (2017) approached Cuba and Florida.

3. Track changes prior to and during TC landfall

As TCs approach land, they may be deflected from their original direction of motion as their circulation interacts with the flow around mountain ranges or complex terrain. Idealized experiments showed that track deflections of systems evolving in the vicinity of Taiwan depend on the angle of approach, the TC size, and the steering flow strength: northwestward-moving TCs approaching to the south of Taiwan slow down and are first deflected southwestward (relative to a without-terrain case) and then northward (Tang and Chan 2014); smaller TCs must move closer to Taiwan to be deflected (Tang and Chan 2015); and larger track deflections occur in weaker easterly steering flows (Tang and Chan 2016; Huang et al. 2016). The southwestward shift is enhanced and the northward deflection is reduced when adding the mainland China terrain to the simulations, suggesting that isolated mountainous islands may have different effects on TC deflection when they are located near larger land masses (Tang and Chan 2014).

Idealized experiments of westward-moving TCs approaching Taiwan highlighted the leading role of the mid-troposphere northerly asymmetric flow in causing the storm southward deflection (Wu et al. 2015). This northerly asymmetric flow forms as a result of the wind speeds restrained east of the storm center and winds enhanced/maintained west of the storm center. This new mechanism occurs in addition to the traditional channeling-effect-induced low-level northerly jet, characterized by low-level wind acceleration over the confined region between the storm center and the Central Mountain Range (CMR). Sensitivity tests indicated that intense TCs experience larger southward deflections prior to landfall when: (i) the CMR terrain is higher (result confirmed by Huang et al. 2016); (ii) the vortex approaches the northern or the middle of the CMR; or (iii) the storm moves slower, i.e. is embedded in a weaker easterly steering flow.

Further investigations of the upstream track deflection of a westward-propagating cyclonic vortex past an isolated mountain range were made using idealized simulations with both boundary layer turbulent mixing and cloud effects (Huang et al. 2016). The direction of upstream track deflection is found to be mainly controlled by the ratio of the vortex size (represented by the radius of the maximum wind RMW) to the north-south length scale of the mountain range (Ly). In addition, the southward deflection distance increases with Ly/RMW. Any reduction in boundary layer turbulent mixing and cloud effects relative to the control values reduced the southward deflection due to weaker channeling effects between the TC circulation and the mountain range.

Since TC motion is affected by the distribution of vorticity and flow around terrain, Lin et al. (2016) used idealized simulations and vorticity budget analyses to examine the orographic influence of a north-south oriented mountain range on track deflection. For a westbound vortex, TC track deflections were explained by: 1) an upstream deceleration due to topographic blocking, which causes a southward deflection of the TC; 2) an anticyclonic motion of the TC as it passes the mountain; and 3) a northwestward movement on the lee slope that may be abrupt (Fig. 2).

These topographical track deflections are important because they may bring a TC closer to a small island with steep mountainous topography; also, they are not restricted to the western North Pacific. The best-track files of Regional Specialized Meteorological Center (RSMC) La Réunion revealed that the tracks of hurricane-strength storms that passed within 380 km of La Réunion island from 1981 to 2015 were also altered and that the steep La Réunion topography generally weakened approaching storms within a 50-km radius (Barbary et al. 2018).

Barbary et al. (2018) also performed a series of idealized simulations of La Réunion's topographical influence with the French non-hydrostatic research model (Meso-NH) at 4-km resolution. As in their observational study, the island effect was more pronounced when the idealized TC was within 100 km of the island. In this scenario, there is: 1) an upstream acceleration, associated with some 7 hPa weakening as 2) the TC is deflected toward the terrain (that weakening is reduced and starts later in the case of a flat island); 3) a deceleration as the TC passes the mountain, which may increase rainfall on the leeward side of the terrain; and 4) an acceleration of the vortex as it moves away from the island. Sensitivity experiments using a TC embedded in a 5 m s^{-1} trade wind flow showed that 6-h observations are theoretically sufficient to detect the terrain effect on the storm translation speed and direction changes when the TC passes within 100 km of La Réunion, as such changes occurred within a 24-h period.

4. Improvements in numerical weather prediction for TC landfall guidance

To implement a numerical model with the high spatial resolution needed to predict the interaction of the TC circulation with the La Reunion topography, and to account for various sources of uncertainty, Météo-France developed a technique to generate ensemble predictions around the RSMC La Réunion official track forecast (Quetelard et al. 2018). First, an ascending hierarchical classification technique was applied to a 5-year sample of RSMC La Réunion forecasts (position and intensity) to identify 40 clusters of typical errors for lead times of 0, 12, 24, 30, 42, 60, and 72 h. Each of the 40 clusters was then assigned a probability according to the number of sample forecasts that compose it. These 40 climatology-based forecasts are considered to represent maximum wind speed and position departures relative to the official RSMC forecast. The European Centre for Medium-Range Weather Forecasts (ECMWF)

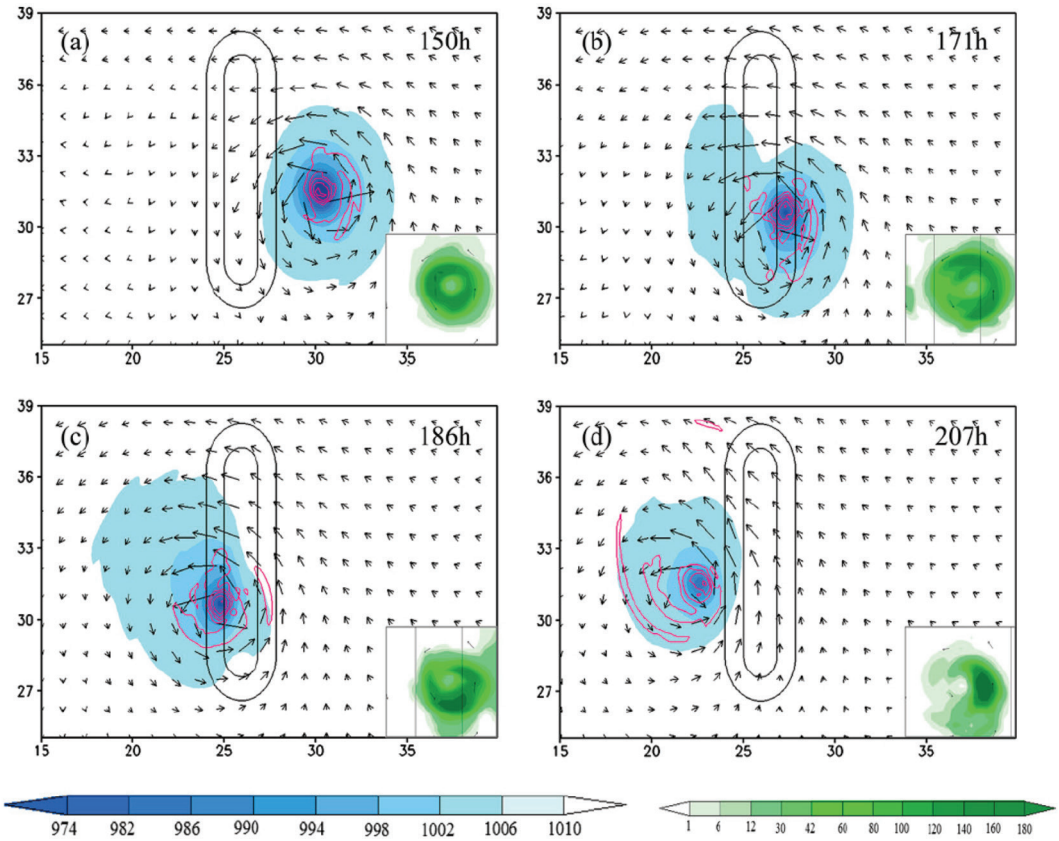

Fig. 2. Track deflection of a westbound TC approaching a north-south oriented mountain range. The 3-h accumulated rainfall is in green, the surface pressure is shaded in blue, and the relative vorticity is contoured in red. Reproduced from Lin et al. (2016).

Ensemble Prediction System (EPS) track forecasts centered on the RSMC official forecast is then considered to account for the event uncertainty. Each of the 51 ECMWF ensemble members is assigned to the nearest climatological cluster based on Euclidean distances, which typically reduces the original set of 40 clusters to about 15 or 30 scenarios depending on the meteorological situation. The probability of each cluster scenario is given by that of the original climatological cluster but weighted according to the number of EPS members that fall in it (e.g., Fig. 3).

For each individual cluster scenario, wind and pressure fields are generated from Meso-NH. A vortex bogus method filters out the short-term forecast TC circulation and inserts a synthetic three-dimensional Holland vortex into the model analysis. The bogus vortex is constructed to fit real-time estimates of storm size and intensity. This high resolution mesoscale ensemble of wind and pressure fields may be used to generate probabilistic products such as the chance of exceeding different wind thresholds (e.g., Fig. 3). This ensemble can also be used to force an ocean surface wave model and/or a storm surge model to provide probabilistic forecasts of oceanic and coastal conditions.

In response to the threat posed by TCs in Taiwan's mountainous terrain, the Taiwan Central Weather Bureau (CWB) recently improved their Typhoon Weather Research and Forecast (TWRF) model (Chen et al. 2017), which is driven by National Centers for Environmental Prediction (NCEP) Global Forecast System (GFS) analyses (Fig. 4). Earlier use of a TC bogus vortex in TWRF resulted in unbalanced fields and large track forecast errors, but the alternative use of "partial cycling" (Hsiao et al. 2012) in TWRF improved the TC initialization. The model is initialized using a "cold start" from t-12 h with a simple interpolation of the GFS fields to the TWRF grid. After a 6-h forward integration of the TWRF model, a "blending scheme" generates a new initial field. The blended scheme is weighted toward the NCEP GFS for scales greater than the cutoff length of 1200 km and toward the TWRF regional field for smaller scales. The large-scale fields from GFS surpass the TWRF analysis, which significantly improves TC track forecasts. On the other hand, the regional TWRF analysis provides a well-developed TC structure and more accurately captures the influence of the Taiwan topography on the TC circulation (Hsiao et al. 2015). The TWRF is then integrated to t =

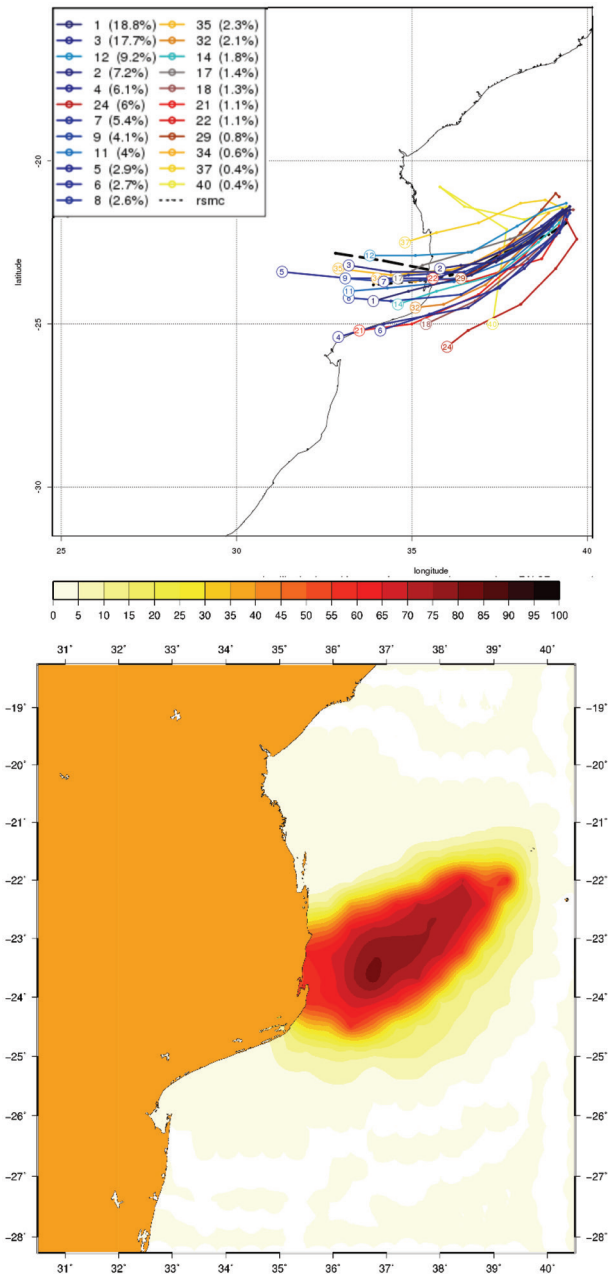

FIG. 3. (Top) Ensemble probabilistic track forecasts initialized at 0000 UTC 14 February 2017 for TC Dineo (2017) making landfall in Mozambique (23 cluster scenarios). (Bottom) Likelihood (%) of winds exceeding a 48-kt threshold in the area for a 60-h period following 0000 UTC 14 February 2017.

0 h, and the blending scheme with the filtered GFS analysis at t = 0 h completes the initialization step. This approach allows a smooth start to the real forecast because the inner-domain fields are dynamically and thermodynamically balanced, and no TC bogus vortex is applied.

A new Fujitsu supercomputer with 92 times the capability of its predecessor further helped model improvement. The new version of TWRF has two domains with finer 15- and 3-km resolutions. Beyond improved representation of the TC inner core, the 3-km grid better resolves the topography of the CMR and land-sea boundaries. The 3-km TWRF domain also encompasses the formation and decay areas of most TCs that might impact Taiwan, the Philippines, and Hong Kong. This expanded coverage motivated PAGASA to request additional CWB guidance products as well as the Hong Kong Observatory to explore installing TWRF on their computer. During the 2017 typhoon season, many TWRF forecasts were more accurate than ECMWF forecasts (Fig. 4a). Increased spatial resolution also helped reduce intensity forecast errors. However, TWRF tends to overpredict intensity, particularly for slow-moving TCs (e.g., Lionrock in 2016), which may be due to the lack of TC-ocean coupling (Fig. 5). CWB is currently testing a one-dimensional upper-ocean mixed-layer model to improve this bias.

Adequate initialization of numerical models is key for accurate predictions of typhoon intensity and structure. Through a WRF-based ensemble Kalman filter (EnKF) data assimilation system, Feng et al. (2017) examined the impacts of assimilating Chinese coastal Doppler radar velocities on the track, intensity, and structure of Typhoons Mujigae (1522), Rammasun (1409) and Meranti (1010). Track errors were reduced in both the EnKF analysis and associated deterministic forecast when more assimilation cycles were used. Offshore enhancement processes in these three cases were also well simulated through cycling radar data assimilation, leading up to a 25 hPa reduction in intensity errors in both the EnKF analysis and prediction compared to an experiment with no data assimilation; The precise structure of the three landfalling typhoons were also closer to observations. An interesting result is that the simulated track, intensity and structure were almost unchanged when restricting the assimilation of radar observations to within 100 km from the typhoon center, which account for about 20% of the total data. On the contrary, the simulated track, intensity and structure were somewhat modified by only assimilating observations within 100-200 km or beyond 200 km from the typhoon center. The strategy of only assimilating inner-core radar data can reduce the computing time to one third, increasing the efficiency of radar assimilation while providing improved operational guidance for typhoon real-time analysis and prediction.

5. Intensity changes prior to and during TC landfall

a. Rapid intensification and rapid decay

While NHC intensity forecasts have improved in recent years (e.g., DeMaria et al. 2014), rapid intensity change (intensity change of at least 30 kt within 24 h) remains a source of error. Rapid intensity changes near land strongly impact coastal preparations as well as the public perception of damage risk, hence the need to further improve intensity

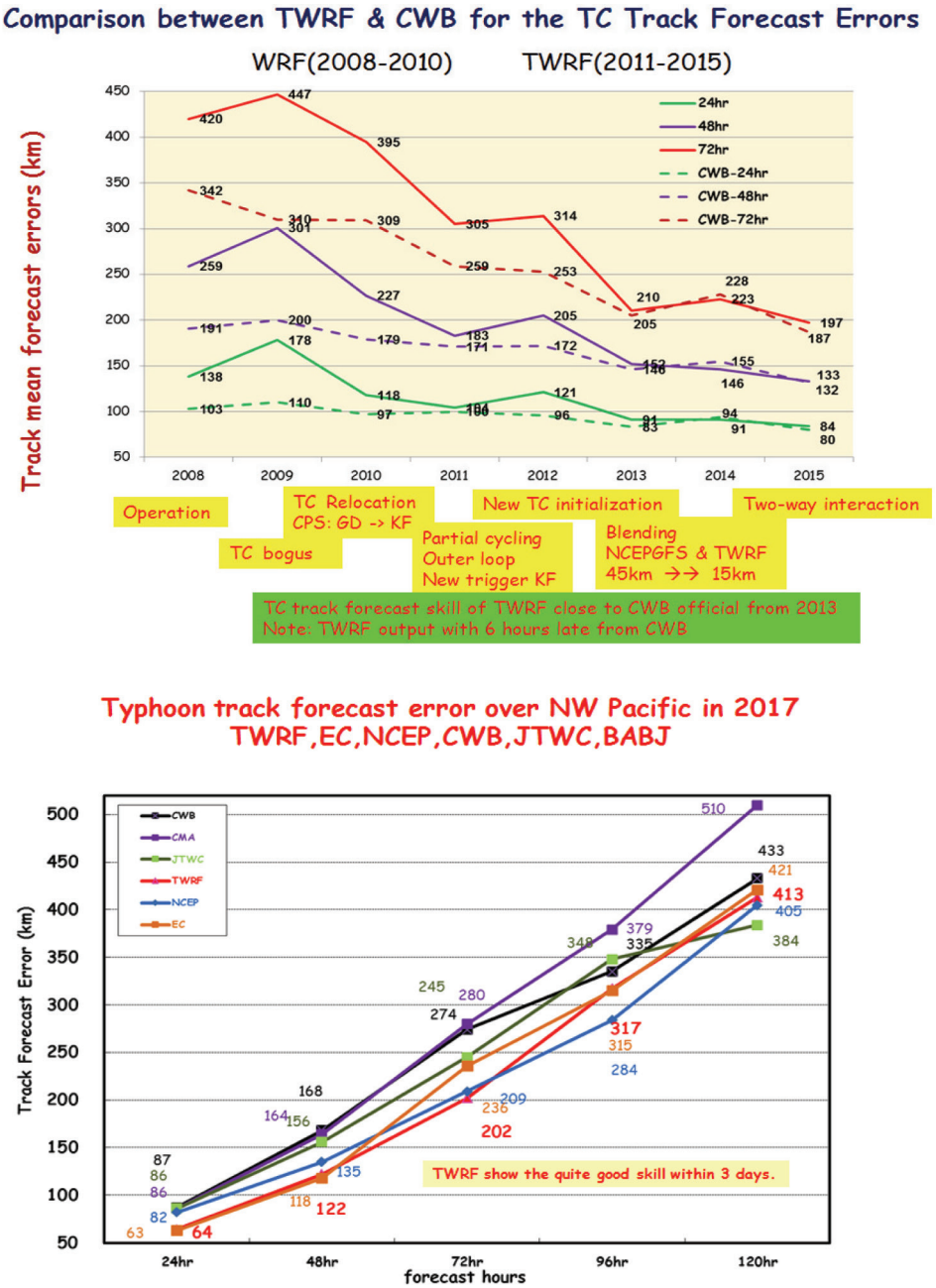

Fig. 4. (Top) Inhomogeneous comparison between TWRF and CWB official TC track forecast errors. Yellow and green highlighted text show the modifications from 2008-2010 (original WRF) to 2011-2015 (TWRF). (Bottom) Comparisons between TWRF, ECMWF, NCEP (GFS), CWB, JTWC, and CMA official track forecast errors in 2017 (through November).

forecasts.

Recent climatological studies of intensity changes and near-land intensity changes have quantified the possible range of TC intensification and decay in different tropical regions. Leroux et al. (2018) established thresholds of rapid intensification (RI) and rapid decay (RD) appropriate for the SWIO using a 17-year climatology based on best track data. Similar to the 30-kt threshold commonly used in the NATL for 1-min sustained wind speeds, RI in the SWIO is defined as a minimum 24-h increase of 15.4 m s^{-1} in the maximum 10-min sustained wind speed. RI in the SWIO occurs more preferably for initial intensities between 65

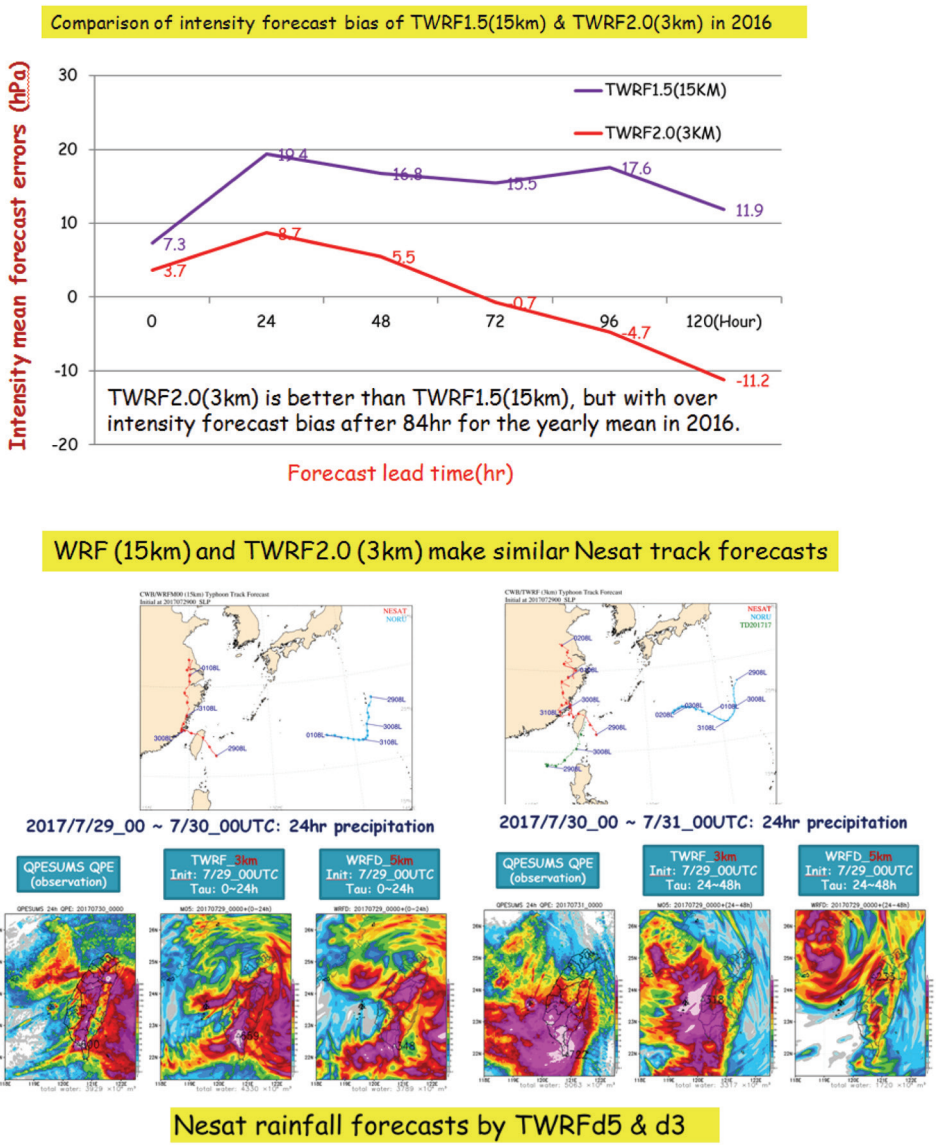

FIG. 5. (Top) Intensity forecast bias of TWRF1.5 (15km) and TWRF2.0 (3km) in 2016. (Bottom) Track and rainfall forecasts for Typhoon Nesat. TWRF2.0 showed more reasonable rainfall structure and distribution than TWRF1.5.

kt and 75 kt. Rapid decay in the SWIO can be defined as a minimum 24-h weakening of 13.9 m s^{-1}, although this threshold may not be appropriate for all systems (tropical depressions or storms or cyclones). Operational intensity forecast errors are shown to be significantly larger for RI events at 24-h lead times (10.8 m s^{-1} versus 4.9 m s^{-1} for non-RI events).

Similar to the SWIO, Xu and Wang (2015) found that the intensification rate of NATL TCs peaks at 70-80 kt (maximum 1-min sustained wind speed). Qin et al. (2016) demonstrated that the intensification rate for NATL hurricanes at the 90th-95th percentile decreases as TC intensity increases from category 3 to category 5. Using best track data from Shanghai Typhoon Institute of the China Meteorological Administration (CMA) for 133 TCs that made landfall in China from 2001 to 2015, Yu et al. (2017) found an average intensity decrease from 34 m s^{-1} before landfall to 20 m s^{-1} 24 h after landfall. Although the average minimum pressure remained steady 6-12 h prior to landfall, rises in minimum pressure did not necessarily follow the changes in maximum wind speed in some cases (Fig. 6), which suggests the wind-pressure relationship may not remain constant during TC landfall. In addition, most TCs that made landfall in China had nearly steady if not increasing intensity prior to landfall and then exhibited the most rapid intensity decrease in the first 6 h after landfall.

Although RI remains a major contributor to intensity forecast errors, rapid decay can also lead to to large er-

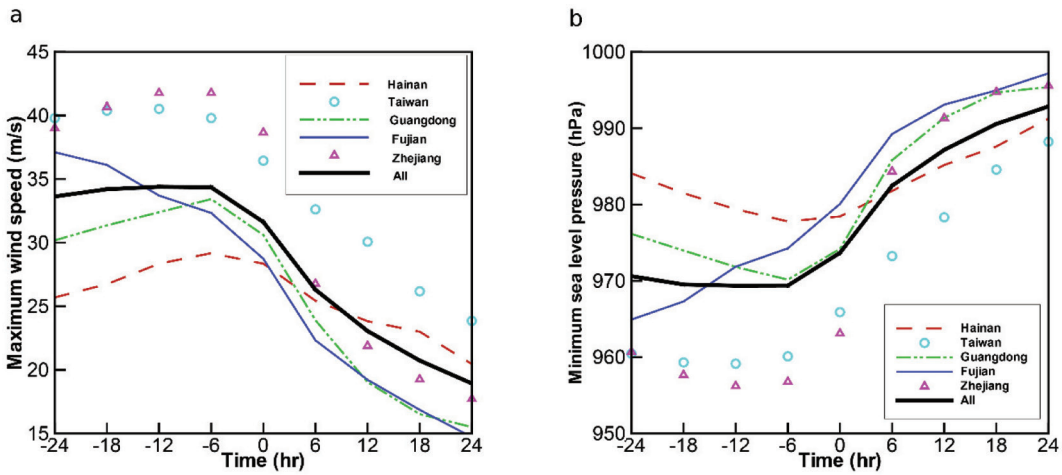

Fig. 6. Best track data for 133 TCs in China showing 6-hourly evolution of (a) the average maximum sustained 10-m wind speed and (b) the average minimum sea level pressure from 24 h prior to landfall to 24 h after landfall. Reproduced from Yu al. (2017).

rors. Using NHC best-track data for the NATL and EPAC, Wood and Ritchie (2015) found greater forecast errors for 24-h RD events compared to slower decay periods. These RD events were associated with negative sea-surface temperature gradients, increasing vertical wind shear, and dry air intrusions. While Wood and Ritchie (2015) focused on weakening when the TC center was at least 50 km from land, these rapid intensity changes can occur closer to land and thus affect both coastal preparation as well as public perceptions of forecast accuracy.

Liang et al. (2016, 2017) applied observational analyses to WNP TCs to demonstrate the contribution of monsoon gyres to RD. For example, Typhoon Chan-Hom (2015) rapidly weakened when it merged with a low-frequency (15-30 days) monsoon gyre. The interaction between these two systems induced the development of strong convection on the eastern side of the monsoon gyre, which prevented inward transport of mass and moisture into the TC and led to the collapse of the eastern part of the eyewall. A composite study showed that more than 40% of RD events south of 25°N in the WNP were observed near the center of monsoon gyres (Liang et al. 2017).

b. Predictions of TC intensity prior to and during landfall

Environmental factors affect TC intensity, such as eddy flux convergence (EFC) of angular momentum and vertical wind shear. Using ECMWF reanalysis data, Peirano et al. (2016) analyzed NATL TCs from 1979 to 2014 and found that trough-induced EFC was a weak predictor of intensity change compared to trough-induced vertical wind shear (Fig. 7). This conclusion may be important for improving intensity predictions of TCs near troughs, particularly if those TCs are also approaching land.

On another hand, sensitivity experiments to vary the initial position and intensity of TC Dora (2007) that interacted with a deep upper-level trough showed that the timing and geometry of the interaction was critical for mid-level PV injection and storm intensification. The variations in environmental forcing relative to the reference simulation illustrated that the relationship between intensity change and the 850–200-hPa wind shear was not systematic and that the 200-hPa divergence, 335–350-K mean potential vorticity, or 200-hPa relative eddy momentum fluxes were better predictors of TC intensification during this TC–trough interaction event (Leroux et al 2016).

Within numerical simulations, horizontal resolution can have a large impact on the predictions of intensity and structure in intense typhoons. Simulations of Typhoon Rammasun (2014) by Wang and Zeng (2017) confirmed that a fine horizontal resolution is crucial to properly resolve inner-core features and improve the forecast of the TC structure and intensity. They also showed that parameterization scheme changes had far smaller impacts than horizontal resolution changes.

The new non-hydrostatic fine-scale model designed specifically for the operational needs of RSMC La Réunion (AROME-IO, Bousquet et al. 2018) has been able to closely predict the extreme intensity variations of Hellen (2014) during experimental tests (Colomb et al. 2018). Based on these simulations and on a few radiosondes, dry air and vertical wind shear at mid levels were found to be the main cause of Hellen's rapid weakening by 90 kt in 24 h. Downdrafts originating at mid levels flushed the inflow layer with low-entropy air. This process contributed to depressed near-core θ_e values, which upset the updrafts in the eyewall. The upper half of the warm core was consistently ventilated by the vertical wind shear, which also contributed to the storm rapid weakening (from hysdrostatic considerations). These

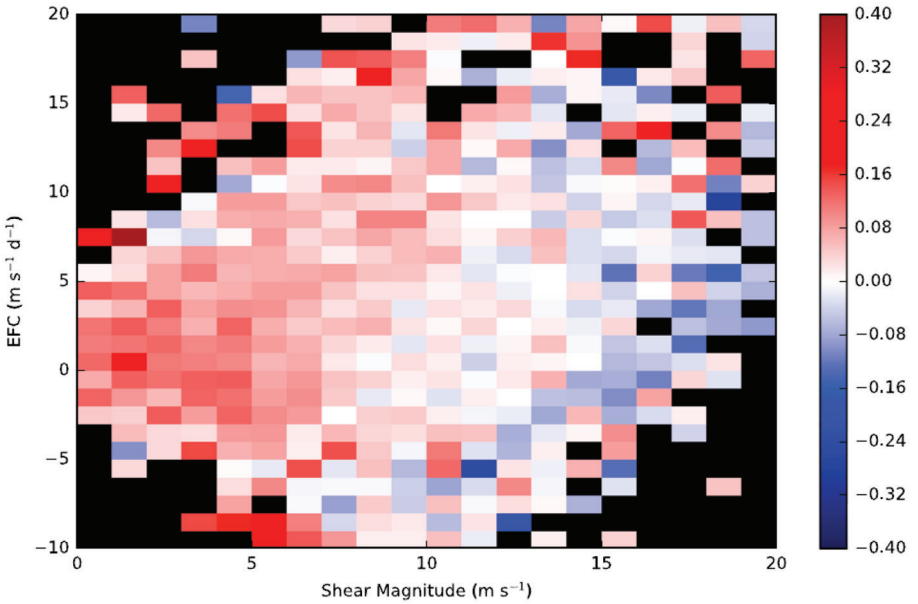

FIG. 7. Mean 24-h dimensionless intensity change (shaded) for all eligible TC periods binned by 850–200 hPa vertical wind shear and 300–600 km eddy flux convergence at 200 hPa. Black indicates no data. Adapted from Peirano et al. (2016).

simulations illustrate for a real TC case the new proposed intensity paradigms for shared TCs that are based on thermodynamic processes (Riemer et al. 2010; Onderlinde and Nolan 2017).

c. Extending TC intensity forecasts to seven days

As the concentration of people and property increases in coastal regions, the requirement for extended lead time and improved accuracy for TC landfall forecasts and warnings becomes increasingly important. Though deterministic and ensemble numerical weather prediction (NWP) models have demonstrated capability for 7-day or longer track forecasts, the capability for TC intensity forecasts remains limited beyond three days. Global NWP models do not have the horizontal grid spacing needed to resolve the inner-core vortex structure and physical processes and at best provide intensity trend forecasts. Regional NWP models better predict TC intensity through greater spatial resolution and improved physical process parameterization, but regional model intensity guidance tends to degrade after 3 days, in part due to degraded TC track forecast accuracy.

Analog approaches employ past TCs with similar characteristics to current events to develop forecasts based on those similarities. Tsai and Elsberry (2014) developed a 5-day Weighted Analog Intensity Pacific (WAIP) technique for WNP TCs using cases with similar tracks and initial intensities to the target TC. By giving higher weights to analogs (past TCs) that best matched the 3-5 day forecast track, they obtained greater accuracy than regional numerical model guidance in 3-5 day forecasts (Tsai and Elsberry 2016). An "ending storm" version was developed (Tsai and Elsberry 2017) to handle landfall, extratropical transition, and delayed development events that were responsible for large intensity over-forecast bias in the 5-7 day interval (Tsai and Elsberry 2015). This modification separately forecasts ending and non-ending storms within the 7-day forecast interval and subsequently reduces forecast error (Fig. 8a,b). To handle shrinking sample sizes at longer forecast lead times, a calibration is used to constrain the spread to 68% within the 12-h WAIP intensity spread values (Fig. 8c,d). In an operational application, the forecaster will need to identify TC landfall within 7 days to allow improved intensity and intensity spread forecast guidance in the case of ending storm events. As the WAIP technique runs in a few minutes on a desktop computer, the forecaster may also easily vary the landfall time to take into account possible along-track forecast errors and see the impacts on the WAIP intensity and intensity spread forecast.

6. Impacts of TC structure and structural changes near land

The Dvorak technique remains the primary method of intensity estimation in basins without regular aircraft reconnaissance, such as the SWIO. Unfortunately, the Dvorak technique is often limited for small TCs. Recent examples of small but intense SWIO TCs include Fantala (2016) and Hellen (2014), which are two of the most intense systems ever recorded in the basin. To address this issue, Leroux et al. (2018) studied the climatological characteristics of midget systems. Over the 2010-2016 period, the

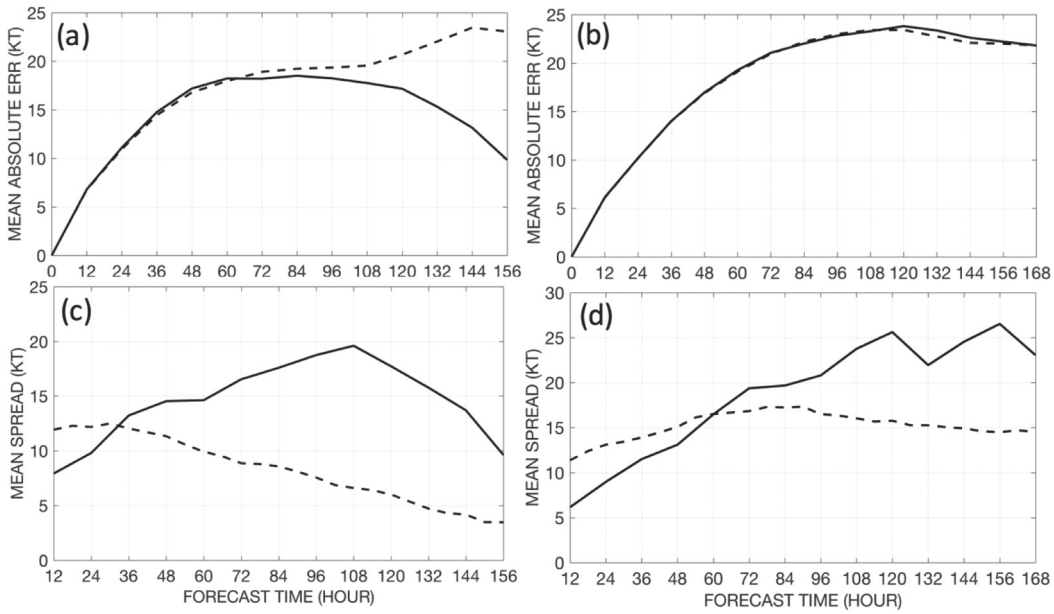

Fig. 8. Mean absolute intensity errors (kt) for independent sets of (a) Ending Storm subsample and (b) Non-ending storm subsample when the separate bias corrections are applied (solid line) or the All Sample (including both ending and non-ending storms) bias corrections are applied (dashed line). (c) and (d) As in panels (a) and (b) except for the mean intensity spreads (kt) before (dashed line) or after (solid line) applying a calibration of the raw intensity spreads to these independent sets.

5th percentile of the 34-kt wind radius (R34) was 46 km, which was then defined as the radius for a midget TC in the SWIO. On average, these midget systems are weaker and have smaller inner cores, which is consistent with their small R34 values. However, midget TCs are more likely to undergo RI and RD, possibly due to greater sensitivity to their environments. A larger midget system sample is needed to assess operational forecast errors regarding the challenge these midget systems represent for intensity and track prediction.

Some efforts have been made to assess TC structural changes near or over land with in situ observations. Kosiba and Wurman (2014) extended Kosiba et al. (2013) by using the Doppler on Wheels (DOW) mobile radar to examine

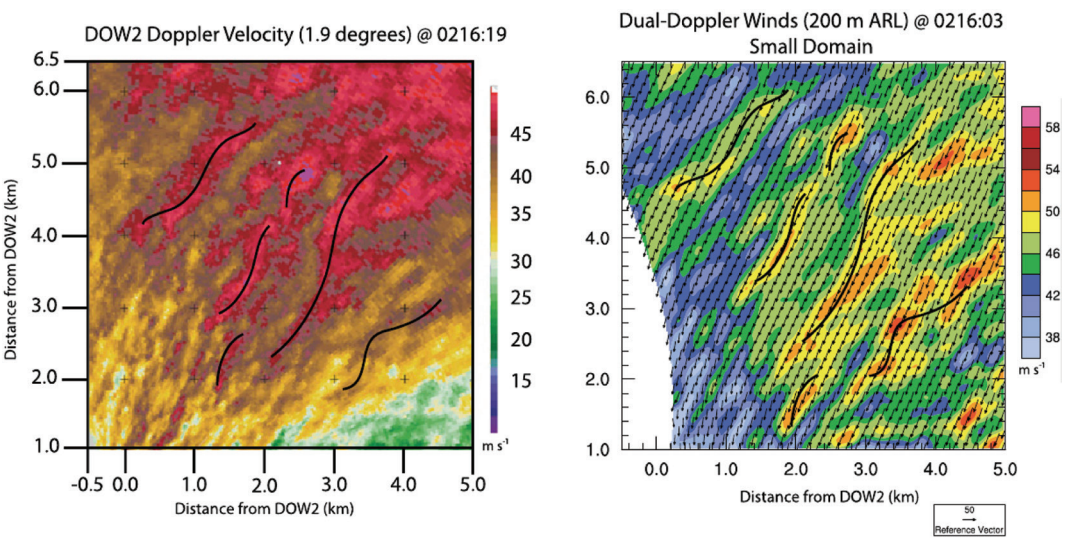

Fig. 9. Magnitude of the (left) raw Doppler velocity data and (right) dual-Doppler synthesis of horizontal winds. Wind streaks are noted by black lines. Reproduced from Kosiba and Wurman (2014).

the boundary-layer structure of Hurricane Frances (2004) at landfall and found linear coherent structures with a characteristic wavelength of 400-500 m (Fig. 9). The vertical flux of horizontal momentum caused by individual vortical structures was substantially higher than values employed in turbulence parameterization schemes. However, the domain-averaged vertical flux was substantially lower than the vertical fluxes in individual vortical structures, which is likely due to the transient nature of the most intense portions of the vortical structures.

Zhang et al. (2017) used numerical simulations to explore the effects of boundary layer vertical mixing in hurricanes over land. For real-case simulations, stronger vertical mixing in the boundary layer at landfall led to improved predictions of track, intensity, and structure. By contrast, weaker vertical mixing resulted in hurricane intensities that were too strong over land. These simulations imply the need to accurately represent vertical mixing in the models to improve forecasts of TCs making landfall.

7. Operational practices and challenges for TC analysis and forecasting

a. Philippine Atmospheric, Geophysical and Astronomical Services Administration (PAGASA)

Operational forecasting is a challenge in the Philippines that is annually impacted by ~20 TCs and their related impacts (i.e., storm surges, strong winds, and heavy precipitation), especially when a TC undergoes rapid changes in intensity and/or moves erratically near the coast. During 2014-2016, 48 TCs impacted the region, and track forecast errors associated with these systems were consistently higher for recurving TCs of lower intensities. Although recurvature forecasts depend on understanding the synoptic-scale environmental flow, which tends to be well predicted, the timing and speed of recurvature can be difficult to accurately predict, particularly for rapid changes in direction.

Tropical Storm Tokage (2016), which was named Marce in the Philippines, is an illustration of the track forecast challenges associated with an abrupt change in direction on 26 November (Fig. 10). Average PAGASA track forecast errors for Tokage were 211, 276, and 546 km at 24, 48, and 72 h, and the bulk of these errors can be attributed to Tokage's unexpected shift to the northeast. Other TC warning centers predicted a shift in the track heading of Tokage (from westward to northwestward or northward), but not the sharp and temporary northeastward turn that preceded a 180-degree shift towards the southwest as they also expected the system to be embedded in the impending cold surge, which would force the TC to move southwestward and weaken.

As indicated in section 5a, forecasting rapid intensity changes is a major challenge. Super Typhoon Haima (2016), known as Lawin in the Philippines, encountered favorable atmospheric and oceanic conditions and rapidly intensified. Unfortunately, PAGASA had predicted no significant intensity changes prior to landfall on Luzon's eastern coast. In response to RI, PAGASA subsequently issued Tropical Cyclone Warning Signal 5, which is the highest value on their warning scale. While Haima continued to intensify just hours prior to landfall, satellite observations revealed the onset of an eyewall replacement cycle (ERC). At the same time, Haima was moving toward a region of strong vertical wind shear (VWS) over Luzon. The combination of decreasing intensity during the first phase of an ERC, strong VWS, and the subsequent interaction of the low-level circulation with mountainous terrain led to Haima weakening much faster than forecast.

b. Joint Typhoon Warning Center (JTWC)

JTWC generates and distributes Significant Tropical Weather Advisories, Tropical Cyclone Formation Alerts, and TC track, intensity, and wind field forecasts for U.S. Government customers in the North Pacific, South Pacific,

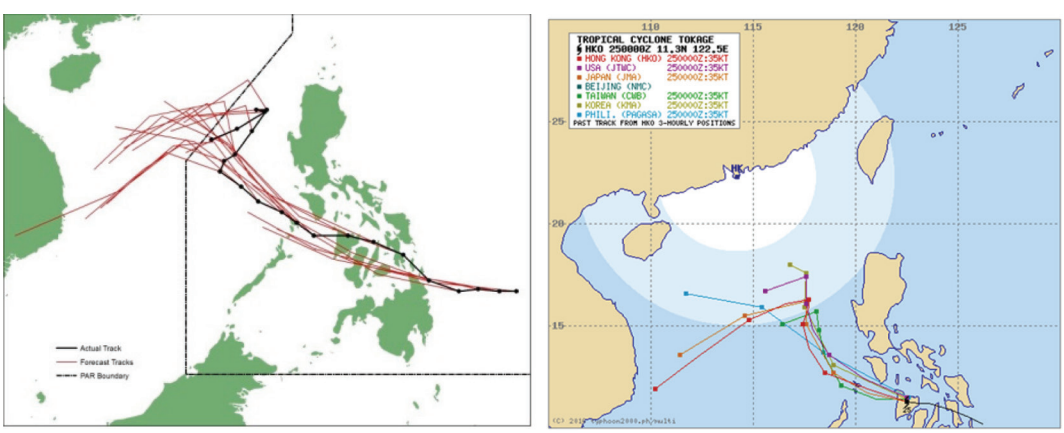

FIG. 10. (Left) 3-day forecast tracks issued by PAGASA through the lifespan of Tropical Storm Tokage. (Right) Forecast tracks of various TC warning centers at 0000 UTC 25 November.

and Indian Ocean basins. Significant Tropical Weather Advisories classify the potential for TC formation from monitored disturbances within a 24-hour forecast period as "low," "medium," or "high". Tropical Cyclone Formation Alerts provide a geographical area for potential TC formation of each disturbance at the "high" classification level. Their TC warnings (issued each 6 h) cover a 120-h forecast period unless either dissipation or extratropical transition (ET) is expected to occur earlier, in which case the JTWC warning will cover the period up to and including the anticipated dissipation or ET. The 1-minute maximum sustained wind speed for initiating TC warnings is 25 kt in the North Pacific and 35 kt in the North Indian Ocean and Southern Hemisphere. However, an "early warning" may be issued below these wind thresholds for timely protection of resources and human life.

The tools and methods that JTWC applies to analyze and forecast TC track, intensity, and structure have been continually improved over the past several years by the transition of several new techniques from applied research into operations. Although satellite observation capabilities have also improved in some respects, there is uncertainty surrounding the future number and observational capabilities of the low-earth orbiting satellites and component sensors.

JTWC forecasters continue to rely upon intensity estimates from the subjective Dvorak technique as well as data from both active and passive satellite sensors and multiple automated, objective intensity estimation techniques. Reliable active scatterometer data provided in near real-time from the Advanced Scatterometer (ASCAT) sensor onboard METOP-A and METOP-B satellites, and more recently from SCATSAT-1, facilitate the intensity analysis process for TCs in the tropical depression and tropical storm stages. Data from these platforms cover large geographic areas that are typically void of reliable *in situ* data.

In addition to subjective Dvorak estimates and scatterometer data, forecasters consider intensity estimates derived from multiple objective methods. These methods include recently introduced intensity estimates that use data from the SSMIS (Hawkins et al. 2016) and ATMS (Herndon and Velden 2016) sensors, the Automated Dvorak Technique (ADT; Olander and Velden 2007) and the automated Satellite Intensity Consensus (SATCON; Velden et al. 2006) provided by the Cooperative Institute for Meteorological Satellite Studies. These automated data are regularly referenced and applied during the intensity analysis process

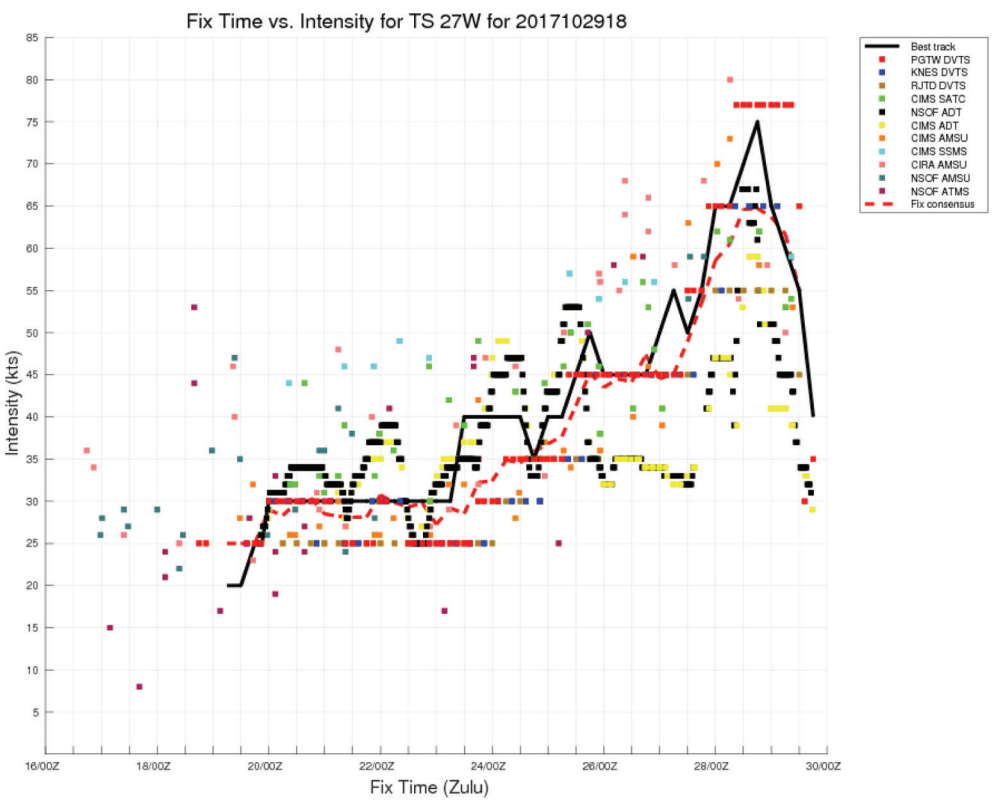

Fig. 11. Example of the intensity time history for TC 27W (2017) showing the intensity estimates currently available to the JTWC forecaster. All estimates listed in the label from "CIMS SATC" (CIMSS SATCON) down are based on automated analysis techniques. These estimates facilitate intensity analysis in open-ocean and near-landfall scenarios alike.

and have been particularly beneficial for identifying and confirming cases of rapid intensity change (Fig. 11). These rapid intensity changes may be otherwise underestimated due to "constraints" inherent to the subjective Dvorak analysis technique and other factors.

JTWC forecasters apply individual guidance products (e.g., statistical-dynamical techniques and dynamical models) and a consensus of these products for forecasting TC intensity. Several new tools and techniques have been introduced at JTWC to both improve intensity prediction and to quantity the potential for rapid intensification. These include probabilistic intensity forecast spreads from the Goerss Predicted Consensus Error (Goerss and Sampson 2014) and WAIP methods (Tsai and Elsberry 2015). By providing upper and lower "bounds" to intensity forecasts, these methods give forecasters insight regarding the potential for rapid intensity change that may not be readily discerned from individual guidance products or the consensus alone. Intensity forecasts from mesoscale model ensembles, such as the COAMPS-TC (Doyle et al. 2012, 2014) ensemble, could further augment and refine available intensity spread guidance. JTWC also employs probabilistic and deterministic rapid intensification guidance (Knaff et al. 2018) based on the Statistical Hurricane Intensity Prediction Scheme (SHIPS; DeMaria et al. 2005) and uses guidance from passive microwave imagery analyses (Kieper and Jiang 2012).

JTWC also now has several new techniques to analyze and forecast TC structure, which should provide more accurate wind guidance during landfall. For example, forecasters now consider an "analysis consensus" (see Sampson et al. 2017 and Fig. 12) composed of satellite-derived automated wind field estimates, dynamic model analysis wind fields, and wind radii derived from the agency's most recent Dvorak intensity fix data (Knaff et al. 2016) when formulating gale force (34-kt) wind radii analyses. Additionally, a consensus of dynamical and statistical-dynamical model surface wind forecasts (Sampson and Knaff 2015) has replaced a climatology and persistence model as the primary tool for wind radii forecasting. Both real-time estimates and forecasts of 34-kt wind radii issued by JTWC have improved following the introduction of these new tools; however, analyzing and forecasting 50- and 64-kt wind radii is more difficult in the absence of high quality observations of the inner core. An increase in remotely sensed observations of the inner core from platforms such as SMAP, SMOS and CYGNSS will surely help in this regard.

c. Australian Bureau of Meteorology (BoM)

Cyclone Marcia (2015) was a strong TC that directly impacted the coast of Queensland, and the model track guidance products were in good agreement regarding the track change near Creal Reef (Fig. 13). However, the intensification of Marcia as it appeared to approach populated and vulnerable locations such as the area of Mackay prompted increased threat messaging for that area at short notice, presumably bearing in mind track errors from past runs and other events and building that into risk calculations for Mackay. The interesting aspect is that Mackay eventually ended up outside the region of gale-force winds (Fig. 13) as originally predicted by NWP models that, in this case, proved to be reasonably accurate about the timing and location of the track change. Questions related to the most effective communication of the forecast guidance are addressed in the companion paper on effective communication and warnings.

d. RSMC La Réunion

Forecasting the intensity of Hellen (2014) was a challenge as it threatened the Comoros archipelago and the Madagascan northwest coastline. Hellen became one of the strongest TCs ever observed in the SWIO. According to RSMC best-track data based on Dvorak estimates (Dvorak 1984), Hellen intensified 70 kt (36 m s^{-1}) in 24 h and reached a peak intensity of 125 kt (64 m s^{-1}) just 132 km from the coast. However, Hellen then rapidly weakened to 90 kt (46 m s^{-1}) in the following 24 hours while remaining over open water. Thus, Hellen made landfall as a weak tropical storm (35 kt). In less than three days, Hellen went up and down the Dvorak scale, as TC forecasters chose to break the Dvorak constraints regarding intensity changes (no more than 2.0 current intensity points in 24 hours) to keep up with the major changes observed in the TC intensity. As discussed in section 6, these rapid intensity variations were facilitated by the TC's small size (Colomb et al. 2018). Hellen had an outermost closed isobar radius at around 220 km, which is about half the climatological mean value in the SWIO (Leroux et al. 2018). These large intensity variations that occurred right before landfall were not well anticipated by operational forecasting models or by the forecasters. Although RI was supported by a generally conducive upper-level environment as well as high ocean heat content in the Mozambique Channel, the record-setting rapid weakening was not supported by usual large-scale predictors.

The uncertainty in the 3-day track forecasts issued by RSMC La Réunion is conveyed using circles of 75% probability around the RSMC official track forecast. These circles are based on the dispersion of cyclone positions in the ECMWF Ensemble Prediction System (EPS), which takes into account the meteorological synoptic context and has proved to be more skillful than using the climatological distribution of track forecast errors (Dupont et al. 2011). All of the potential coastal impacts (e.g., devastating winds, torrential rain, marine and river inundations) are tightly related to the storm track as well as the TC structure and intensity evolutions. Therefore, risk managers or public agencies need both a reliable forecast of the intensity evolution and an estimation of the intensity uncertainty (e.g., probability that the intensity will exceed a certain threshold).

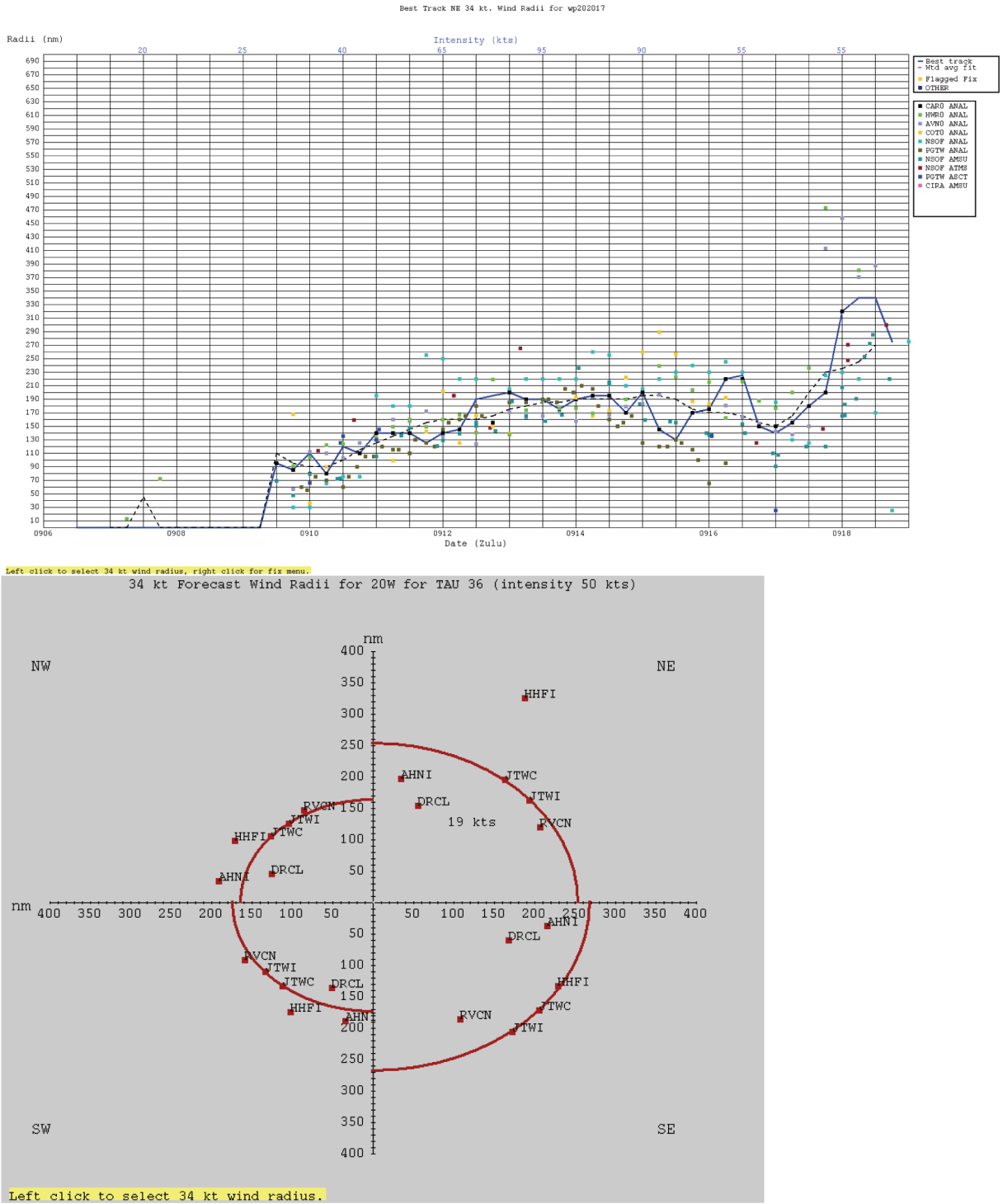

FIG. 12. Example for TC 20W (2017) of (Top) wind radii analysis time history showing the various estimates and objective consensus values available to the forecaster and (Bottom) wind radii forecast plot showing forecaster-selected 34-kt wind radii by quadrant along with wind radii forecast consensus component model and other estimates.

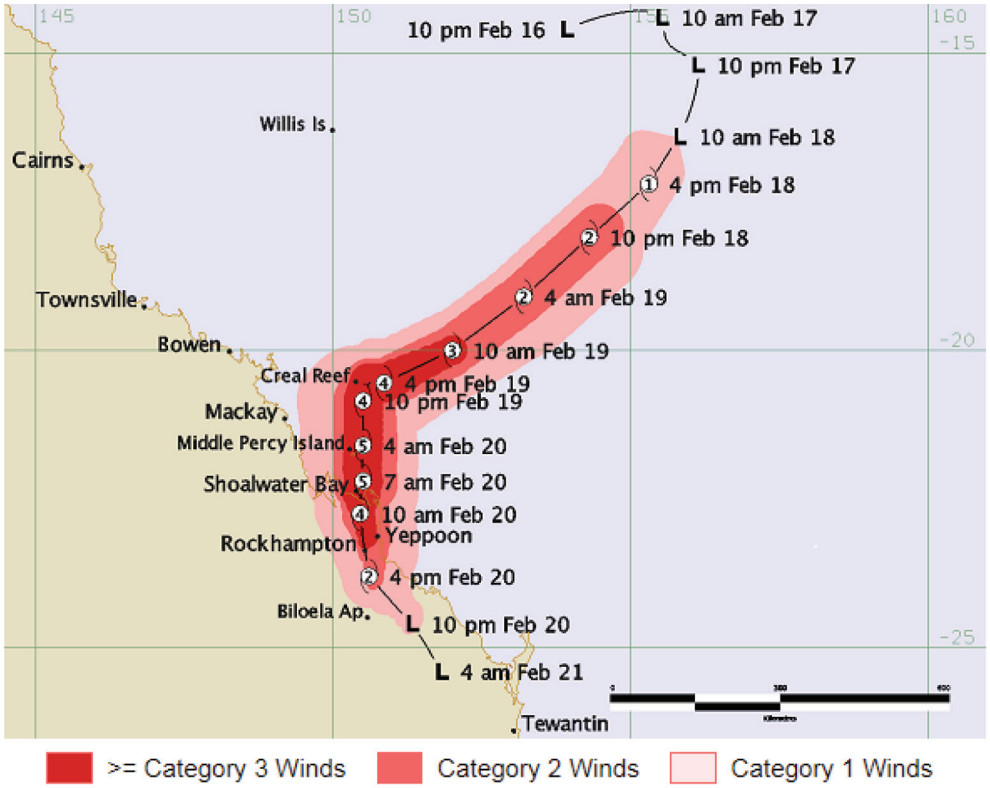

FIG. 13. Track of severe tropical cyclone Marcia (2015), showing estimated areas affected by winds associated with given categories of cyclone intensity (shaded contours). Adapted from http://www.bom.gov.au/cyclone/history/marcia.shtml.

This is the reason why Météo-France has now developed a technique to generate ensemble predictions around the RSMC La Réunion official forecast for both the TC track and intensity (section 4) as well as for other parameters such as the storm surge and waves.

Additional intensity guidance is provided to SWIO forecasters with the first empirical Maximum Potential Intensity-Sea Surface Temperature (MPI-SST) relationship developed specifically for the SWIO basin. This parameter is derived in the 22-29°C range using best-track data and daily optimally interpolated SST (OISST) analyses at 0.25° latitude-longitude resolution (Leroux et al. 2018). This empirical MPI implicitly includes the effect of the TC outflow temperature on storm intensity. The exponential function differs from the MPIs derived for the NATL and WNP (Zeng et al. 2007; Gao et al. 2016), and from the nearly linear relationships utilized in the ENP and the Bay of Bengal. The 29°C cutoff reflects the unique features of the Mozambique Channel that spawns systems over very warm waters (compared to the open ocean) but these systems have very little time to intensify before making landfall.

Another intensity guidance product for the SWIO is being developed that will use sophisticated statistical techniques (e.g., neural network, decision trees, and multilinear regression of the most relevant environmental predictors). This new statistical-dynamical product will be patterned after those developed in other basins (e.g., DeMaria and Kaplan 1994; Knaff et al. 2005; Kaplan et al. 2010; Gao and Chiu 2012) and will provide short-range prediction of both TC intensity and RI probability.

Track deflections imposed by nearby terrain remain a forecast challenge in the SWIO. For example, Cyclone Enawo (2017) jogged to the northwest shortly before landfall, which was a track change that was not forecast by RSMC La Réunion. Consequently, this track shift resulted in the Enawo track being outside the 75% cone of uncertainty for that RSMC La Réunion track forecast (Fig. 14). Unfortunately, this intense cyclone caused at least 81 deaths and USD $20 million in damage.

8. Summary and potential for future research

Sections 2 to 7 are summarized in a comprehensive map that highlights the recent advances, challenges, knowledge gaps and suitable research routes on the topic of rapid changes in TC track, intensity, and structure at or near landfall (Fig. 16).

The report highlighted a number of recent advances in observing TCs. Higher resolution imagers on next-gener-

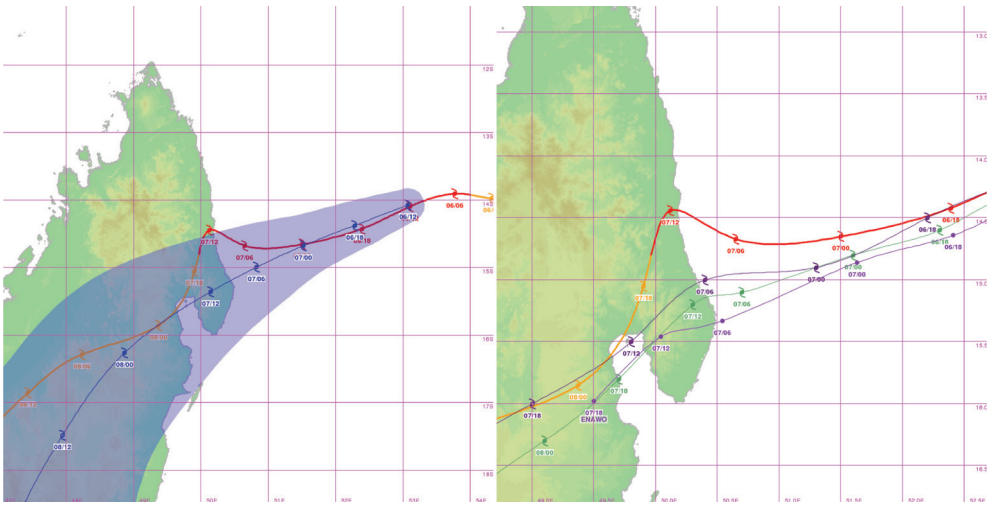

Fig. 14. (Left) Best track (red) and RSMC La Réunion official track forecast (blue) at 1200 UTC 06 March 2017 with EPS-based uncertainty circles of 75% probability (shaded area) for TC Enawo. (Right) Track forecasts from 0000 UTC 06 March 2017 for three numerical models: Arome-IO at 2.5-km resolution (light purple; southernmost track), GFDN (green), and HWRF (deep purple).

ation geostationary satellites (Himawari-8 and GOES-16) are already assisting forecasters, and a new constellation of low-earth orbiting satellites such as CYGNSS are expected to provide useful information on TC size and structure. Unfortunately, an anticipated decrease in the number of LEO satellites carrying high-resolution microwave sounders and infrared imagers suitable for observing TCs will hinder all forecast agencies' capability to accurately analyze TC positions and detect rapid track changes. The development and deployment of satellites that carry these sensors and systems and provide their data through accessible outlets in near real-time is a high priority. Ongoing experiments with constellations of small satellites, such as TROPICS (https://tropics.ll.mit.edu/CMS/tropics/Mission-Overview), offer a potential framework for providing economical, high frequency microwave sensor coverage of TCs in the years ahead. Given forecasters' experiences with microwave-derived and/or automated satellite intensity estimates such as the ADT, continued progress in the development and refinement of automated TC intensity analysis is essential. In addition, we need to take advantage of improving observations from geostationary satellites due to their temporal coverage of large regions at risk of TC landfall. Of course, higher density in situ observations are also highly desired for both real-time analysis and verification.

Track deflections for systems near complex topography such as Taiwan and La Réunion have been further investigated, and increased awareness of the dynamics behind these events may improve future forecasts. Intensity change remains a challenge, with multiple recent examples of short-term intensity change near land causing difficulty, but refinements in some NWP models and the use of probabilistic forecasts shall help for delivering effective communication and warnings in future similar events. An analog technique was developed to extend intensity forecast guidance from 3 to 7 days, exploiting the improved capability in track forecasts at long lead times (> 5 days). This technique shall provide more time for evacuations and would allow disaster preparedness activities to be completed.

Many advances in understanding, observing, and predicting TCs have originated as a result of field experiments in the NATL and EPAC basins over many years. Similar TC-related field campaigns are needed to provide insights and refinements to the TC observing systems in the SWIO. In that regard, considerable efforts are currently being made to improve TC observation systems in this particular basin through deploying new atmospheric and oceanic sensors. An example is the SWIO-TC experiment to be organized in the Mozambique Channel and Mascarene Archipelago in 2019. This field campaign under the EU-funded ReNov'Risk-Cyclones project will provide unprecedented atmospheric and oceanic datasets in the SWIO basin. The scientific objectives are to: i) better understand the physics of TCs over the SWIO and the relationships between TCs and the large-scale atmospheric and oceanic environment; ii) specifically calibrate for the SWIO the multiple satellite techniques, such as the Dvorak technique, that are dedicated to TC detection and forecasting; iii) objectively estimate TC forecast improvements due to the assimilation of additional data from surface stations, airborne measurements, and satellite observations; and iv) test the capabilities of high-resolution numerical models to reliably predict the evolution of TC wind and precipitation structures as well as to predict their impacts on the coastal regions of the SWIO.

Although quantitative guidance for predicting TC rapid intensification events is improving, more specific forecasts regarding the timing and extent of intensification are required, particularly for landfalling systems. Techniques to identify and isolate high probability extreme events—for example, intensification of at least 50 kt within a 24-h period—could mitigate losses in potentially catastrophic prelandfall rapid intensification events (Fig. 15). In addition, rapid intensity changes are not limited to the 24-h timeframe. Other timeframes should be considered in all basins, but shorter timeframes require observations at greater temporal resolution.

Many of these TC forecast challenges can be addressed using improved remotely-sensed observations and derived parameters such as high spatial and temporal resolution atmospheric motion vectors. However, the challenge is to assimilate these new datasets into high-resolution ensemble prediction systems. The use of coupled statistical-dynamical approaches can also help improve the accuracy of TC intensity predictions. In addition, increased computing power and improved numerical weather prediction models show promise in better characterizing TC structure and subsequently producing more accurate intensity forecasts.

After all the participants of the IWTCLP-IV were able to discuss the topic presented here, i.e., rapid changes in track, intensity, and structure at landfall, a set of recommendations was submitted to the WMO and merged with those from other topics. These recommendations are directed at the TC operational community, TC research community, the integrated TC operational and research community, and the WMO itself. They are provided in a companion paper that describes the IWTCLP-IV workshop.

Acknowledgments

Preparation of this report for IWTCLP-4 greatly benefited from discussions within the workshop and from input by members of the working group on track, intensity, and structure change not listed as co-authors here: Nancy Baker (NRL-Monterey), Difei Deng (UNSW-Canberra and IAP), Jia Liang (Nanjing University of Information Science and Technology), Kuo-Chen Lu (Taiwan Central Weather Bureau), Nanan Qin (Nanjing University of Information Science and Technology), Hsiao-Chung Tsai (Tamkang University), and Liguang Wu (Nanjing University of In-

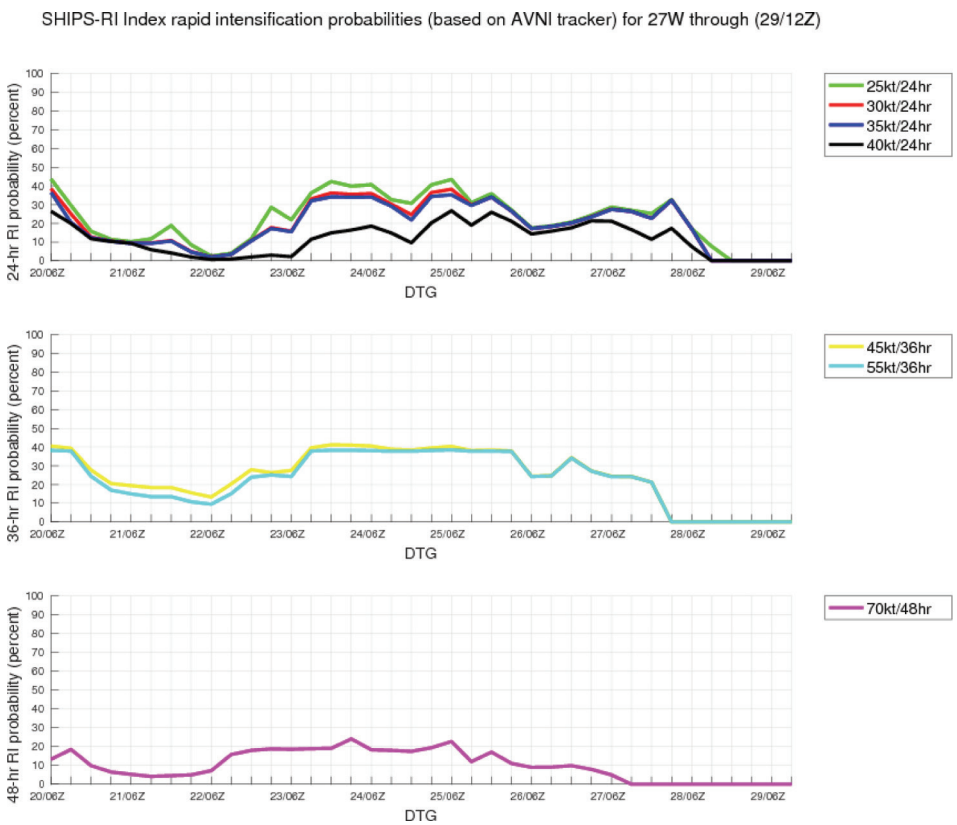

FIG. 15. Example graphic for TC 27W (2017) showing changes in SHIPS-RI rapid intensification probabilities for the listed thresholds and timeframes. Although these data significantly aid short range predictions of rapid intensity change, additional methods to forecast the timing and extent of rapid intensity change with greater specificity and to identify the potential for extreme events are still needed.

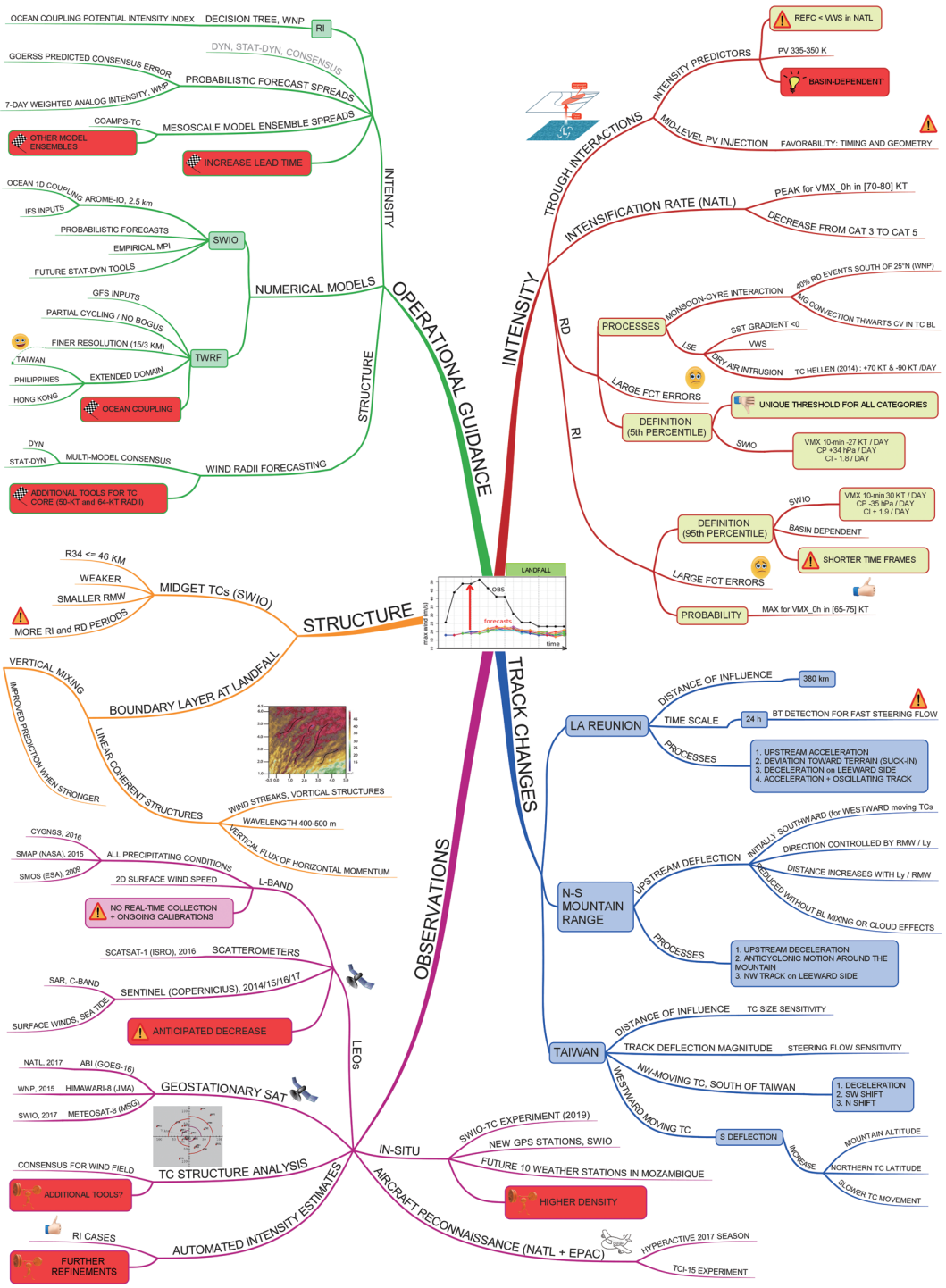

Fig. 16. Comprehensive map showing the recent advances, challenges and possible future routes on the problem of TC track, intensity and structure changes at or near landfall. The BL stands for boundary layer, CI for current intensity, CP for central pressure, CV for convergence, DYN for dynamical, EPAC for eastern North Pacific, FCT for forecast, LSE for large-scale environment, Ly the north-south (N-S) length scale of a N-S oriented mountain range, MG for monsoon gyre, MPI for maximum potential intensity, N for northward, NATL for North Atlantic, NW for northwestward, PV for potential vorticity, RD for rapid decay, REFC for relative eddy momentum flux convergence, RI for rapid intensification, RMW for radius of maximum wind, S for southward, SST for sea surface temperature, STAT for statistical, SW for southwestward, SWIO for southwest Indian Ocean, TC for tropical cyclone, VMX for maximum wind speed, VWS for vertical wind shear, and WNP for western North Pacific.

formation Science and Technology). Penny Jones provided excellent assistance in the preparation of the manuscript. The co-authorship order after the first three authors is determined by the surnames and not by the degree of author contribution.

References

Barbary, D., O. Bousquet, and M.D. Leroux, 2018: The orographic effect of Réunion island on tropical cyclone track and intensity. *In prep. for Atmos. Sci. Lett.*

Bousquet O., D. Barbary, S. Bielli, G. Faure, T. Montmerle, P. Brousseau and Q.-P. Duong, 2018: AROME-IO: A new tool for high resolution modeling of tropical cyclones in the SW Indian Ocean. Submitted to *Journal of Advances in Modeling Earth Systems*.

Chen, D.-S. , L.-F. Hsiao, T.-C. Yeh, C.-T. Cheng, C.-T. Fong, and J.-S. Hong, 2017: Impact of the TWRF model resolutions on tropical cyclone track, intensity and rainfall predictions over the western North Pacific. *Asia Oceania Geosciences Society (AOGS) 14th Annual Meeting*, 6-12 August, 2017, Singapore, AS17-D3-PM1, p221.

Cheung, K., 2014: Track, structure, and intensity changes at landfall. Topic 6. International Workshop on Tropical Cyclone Landfall Processes. [Available athttp://www.wmo.int/pages/prog/arep/wwrp/new/IWTC8_Pre-WorkshopDocs.html]

Colomb, A., T. Kriat, and M.D. Leroux, 2018: The rapid weakening of Very Severe Tropical Cyclone Hellen (2014). *In prep. for J. Atmos. Sci.*

DeMaria, M., and J. Kaplan, 1994: A Statistical Hurricane Intensity Prediction Scheme (SHIPS) for the Atlantic basin. *Wea. Forecasting*, **9**, 209–220.

DeMaria, M., M. Mainelli, L.K. Shay, J.A. Knaff, and J. Kaplan, 2005: Further improvements to the Statistical Hurricane Intensity Prediction Scheme (SHIPS). *Wea. Forecasting*, **20**, 531–543, https://doi.org/10.1175/WAF862.1.

DeMaria, M., C.R. Sampson, J.A. Knaff, and K.D. Musgrave, 2014: Is tropical cyclone intensity guidance improving? *Bull. Amer. Met. Soc.*, **95**, 387-398.

Doyle, J. D., Y. Jin, R.M. Hodur, S. Chen, H. Jin J. Moskaitis, A. Reinecke, P. Black, J. Cummings, E. Hendricks, T. Holt, C.-S. Liou, M. Peng, C. Reynolds, K. Sashegyi, J. Schmidt, and S. Wang, 2012: Realtime tropical cyclone prediction using COAMPS-TC. *Advances in Geosci.*, **28**, 15-28, doi:10.1142/9789814405683_0002.

Doyle, J.D., R. M. Hodur, S. Chen., Y. Jin, J. R. Moskaitis, S. Wang, E. A. Hendricks, H. Jin, and T. A. Smith, 2014: Tropical cyclone prediction using COAMPS-TC. Oceanography 27(3):104–115, http://dx.doi.org/10.5670/oceanog.2014.72.

Doyle, J. D., and 31 co-authors, 2017: A view of tropical cyclones from above: The Tropical Cyclone Intensity Experiment. *Bull. Amer. Meteor. Soc.,* **98**, 2113-2134.

Dupont, T., M. Plu, P. Caroff, and G. Faure, 2011: Verification of ensemble-based uncertainty circles around tropical cyclone track forecasts. *Wea. Forecasting*, **26**, 664–676.

Dvorak, V. F., 1984: Tropical cyclone intensity analysis using satellite data. NOAA Tech. Rep. 11, 45 pp.

Feng J. N., Duan Y. H., Xu J. Improving the Simulation of Typhoon Mujigae (2015) Based on Radar Data Assimilation. *Journal of applied meteorological science*, 2017, **28**, 399–413.

Gao, S., and L. S. Chiu, 2012: Development of statistical typhoon intensity prediction: Application to satellite observed surface evaporation and rain rate (STIPER). *Wea. Forecasting*, **27**, 240–250.

Gao, S., W. Zhang, J. Liu, I.-I. Lin, L. S. Chiu, and K. Cao, 2016: Improvement in typhoon intensity change classification by incorporating an ocean coupling potential intensity index into decision trees. *Wea. Forecasting*, **31**, 95-106.

Goerss, J.S. and C.R. Sampson, 2014: Prediction of consensus tropical cyclone intensity forecast error. *Wea. Forecasting*, **29**, 750–762.

Hawkins, J., D.C. Herndon, and C.S. Velden, 2016: SSMIS tropical cyclone monitoring opportunities**.** Preprints, *32nd Conference on Hurricanes and Tropical Meteorology*, San Juan, PR, Amer. Meteor. Soc.

Herndon, D. and C.S. Velden, 2016: Estimation of tropical cyclone intensity using the CIMSS ATMS tropical cyclone intensity algorithm. *21st Conference on Satellite Meteorology, Oceanography, and Climatology*, Madison, WI, Amer. Meteor. Soc.

Hsiao, L. F., D.-S. Chen, Y.-H. Kuo, Y.-R. Guo, T.-C. Yeh, J.-S. Hong, C.-T. Fong, and C.-S. Lee, 2012: Application of WRF 3DVAR to operational typhoon prediction in Taiwan: impact of outer loop and partial cycling approaches. *Wea. Forecasting*, **27**, 1249-1263.

Hsiao, L. F., X.-Y. Huang, Y.-H. Kuo, D.-S. Chen, H. Wang, C.-C. Tsai, T.-C. Yeh, J.-S. Hong, C.-T. Fong, C.-S. Lee, 2015: Blending of global and regional analyses with a spatial filter: Application to typhoon prediction over the western North Pacific Ocean. *Wea. Forecasting*, **30**, 754-770.

Huang, C.-Y., C.-A. Chen, S.-H. Chen, and D. S. Nolan, 2016: On the upstream track deflection of tropical cyclones past a mountain Range: Idealized experiments. *J. Atmos. Sci*. **73**, 3157-3180.

Kaplan, J., M. DeMaria, and J. A. Knaff, 2010: A revised tropical cyclone rapid intensification index for the Atlantic and eastern North Pacific basins. *Wea. Forecasting*, **25**, 220–241.

Kieper, M. and H. Jiang, 2012: Predicting tropical cyclone rapid intensification using the 37 GHz ring pattern identified from passive microwave measurements. *Geophys. Res. Lett*., **39**, L13804.

Knaff, J. A., C. R. Sampson, and M. DeMaria, 2005: An operational Statistical Typhoon Intensity Prediction Scheme for the western North Pacific. *Wea. Forecasting*, **20**, 688–699.

Knaff, J. A., C. J. Slocum, K. D. Musgrave, C. R. Sampson, and B. R. Strahl, 2016: Using routinely available information to estimate tropical cyclone wind structure. *Mon. Wea. Rev.*, **144**, 1233-1247.

Knaff, J. A., C. R. Sampson, and G. Chirokova, 2017: A global statistical-dynamical tropical cyclone wind radii forecast scheme. *Wea. Forecasting,* **32,** 629–644, doi: 10.1175/WAF-D-16-0168.1.

Knaff, J. A., C. R. Sampson, and K. Musgrave, 2018: An Operational Rapid Intensification Prediction Aid for the western North Pacific. *Wea. Forecasting,* submitted.

Kosiba, K. A., and J. Wurman, 2014: Finescale dual-Doppler analysis of hurricane boundary layer structures in Hurricane Frances (2004) at landfall. *Mon. Wea. Rev.,* **142**, 1874-1891.

Kosiba, K. A, J. Wurman, F. J. Masters, and P. Robinson, 2013: Mapping of near-surface winds in Hurricane Rita using finescale radar, anemometer, and land-use data. *Mon. Wea. Rev.*, **141**, 4337-4349.

Leroux, M.-D., M. Plu, and F. Roux, 2016: On the Sensitivity of Tropical Cyclone Intensification under Upper-Level Trough Forcing. *Mon. Wea. Rev.*, **144**, 1179-1202, doi: 10.1175/MWR-D-15-0224.1

Leroux, M.-D., J. Meister, D. Mekies, A.-L. Dorla, and P. Caroff, 2018: A Climatology of Southwest Indian Ocean Tropical Systems: their Number, Tracks, Impacts, Sizes, Empirical Maximum Potential Intensity and Intensity Changes. *J. Appl. Meteor. Climatol.*, doi:10.1175/JAMC-D-17-0094.1, in press.

Liang, J., L. Wu, G. Gu, and Q. Liu, 2016: Rapid weakening of Typhoon Chan-Hom (2015) in a monsoon gyre. *J. Geophys.*

Res. Atmos., **121**, 9508-9520, doi: 10.1002/2016JD025214.

Liang, J., L. Wu, and G. Gu, 2018: Numerical study of the influences of a monsoon gyre on intensity changes of Typhoon Chan-Hom (2015), *Advances in Atmospheric Sciences*, **35**, 567-579, doi:10.1007/s00376-017-7155-6.

Lin, Y.-L., S.-H. Chen, and L. Liu, 2016: Orographic influence on basic flow and cyclone circulation and their impacts on track deflection of an idealized tropical cyclone. *J. Atmos. Sci.,* **73**, 3951-3974.

Meissner, T., L. Ricciardulli, and F. Wentz, 2017: Capability of the SMAP mission to measure ocean surface winds in storms. *Bull. Amer. Meteor. Soc.*, 98, 1660-1677, doi: https://doi.org/10.1175/BAMS-D-16-0052.1.

Morris, M. and C. S. Ruf, 2017: Determining tropical cyclone surface wind speed structure and intensity with the CYGNSS satellite constellation. *J. Appl. Meteor. Climatol.*, 56, 1847-1865, doi: 10.1175/JAMC-D-16-0375.1.

Olander, T. L. and C. S. Velden, 2007: The Advanced Dvorak Technique: Continued development of an objective scheme to estimate tropical cyclone intensity using geostationary infrared satellite imagery. *Wea. Forecasting*, **22**, 287-298.

Onderlinde, M. J., and D. S. Nolan, 2017: The tropical cyclone response to changing wind shear using the method of time-varying point-downscaling. *Journal of Advances in Modeling Earth Systems*, doi:10.1002/2016MS000796.

Peirano, C. M., K. L. Corbosiero, and B. H. Tang, 2016: Revisiting trough interactions and tropical cyclone intensity change. *Geophys. Res. Lett.*, **43**, 5509–5515.

Podlaha, A., S. Bowen, C. Darbinyan, and M. Lörinc, 2017: Global Catastrophe Recap - April 2017. Aon Benfield Analytics, 13 pp.

Qin, N., D.-L. Zhang, and Y. Li, 2016: A statistical analysis of steady eyewall sizes associated with rapidly intensifying hurricanes. *Wea. Forecasting*, **31**, 737-742.

Quetelard, H. M., F. D. Bonnardot, G. D. Jumaux, and M. Bessafi, 2018. Probabilistic forecasts of tropical cyclone track and intensity through ensemble techniques. In prep. for *Quart. J. Roy. Meteor. Soc.*

Reul, N., B. Chapron, E. Zabolotskikh, C. Donion, A. Mouche, J. Tenerelli, F.Collard, J. Piolle, A. Fore, S. Yueh, J. Cotton, P. Francis, Y. Quilfen, and V.Kudryavtsev, 2017: A new generation of Tropical Cyclone Size measurements from space. *Bull. Amer. Meteor. Soc.*, doi:10.1175/BAMS-D-15-00291.1, in press.

Riemer, M., M. T. Montgomery, and M. E. Nicholls, 2010: A new paradigm for intensity modification of tropical cyclones: Thermodynamic impact of vertical wind shear on the inflow layer. *Atmos. Chem. Phys.*, **10**, 3163-3188.

Rogers, R., S. Aberson, A. Aksoy, B. Annane, M. Black, J. Cione, N. Dorst, J. Dunion, J. Gamache, S. Goldenberg, S. Gopalakrishnan, J. Kaplan, B. Klotz, S. Lorsolo, F. Marks, S. Murillo, M. Powell, P. Reasor, K. Sellwood, E. Uhlhorn, T. Vukicevic, J. Zhang, and X. Zhang, 2013: NOAA'S Hurricane Intensity Forecasting Experiment: A Progress Report. *Bull. Amer. Meteor. Soc.*, **94**, 859–882.

Rogers, R. F., S. Aberson, M.M. Bell, D. J. Cecil, J. D. Doyle, T. B. Kimberlain, J. Morgerman, L. K. Shay, and C. Velden, 2017: Rewriting the tropical record books: The extraordinary intensification of Hurricane Patricia (2015). *Bull. Amer. Meteor. Soc.*, **98**, 2091-2112.

Sampson, C.R. and J. A. Knaff, 2015: A consensus forecast for tropical cyclone gale wind radii. *Wea. Forecasting*, **30**, 1397-1403.

Sampson, C. R., E. M. Fukada, J. A. Knaff, B. R. Strahl, M. J. Brennan, T. Marchok, 2017: Tropical cyclone gale wind radii estimates for the western North Pacific. *Wea. Forecasting,* 32**,** 1007-1028, doi:10.1175/WAF-D-16-0196.1.

Schmit, T. J., P. Griffith, M. M. Gunshor, J.M. Daniels, S. J. Goodman, and W. J. Lebair, 2017: A closer look at the ABI on the GOES-R series. *Bull. Amer. Met. Soc.*, **98**, 681-698.

Tang, C. K., and J. C. L. Chan, 2014: Idealized simulations of the effect of local and remote topographies on tropical cyclone tracks. *Q. J. Royal Meteorol. Soc.*, **141**, 2045-2056.

Tang, C. K., and J. C. L. Chan, 2015: Idealized simulations of the effect of Taiwan topography on the tracks of tropical cyclones with different sizes. *Q. J. Royal Meteorol. Soc.*, **142**, 793-804.

Tang, C. K., and J. C. L. Chan, 2016: Idealized simulations of the effect of Taiwan topography on the tracks of tropical cyclones with different steering flow strengths, *Q. J. Royal Meteorol. Soc.*, **142**, 3211-3221.

Tsai, H.-C., and R. L. Elsberry, 2014: Applications of situation-dependent intensity and intensity spread predictions based on a weighted analog technique. *Asia-Pacific J. Atmos. Sci*., **50**, 507-518.

Tsai, H.-C., and R. L. Elsberry, 2015: Seven-day intensity and intensity spread predictions for western North Pacific tropical cyclones. *Asia-Pacific J. Atmos. Sci*., **51**, 331-342.

Tsai, H.-C., and R. L. Elsberry, 2016: Skill of western North Pacific tropical cyclone intensity forecast guidance relative to weighted-analog technique. *Asia-Pacific J. Atmos. Sci*., **52**, 281-290.

Tsai, H.-C., and R. L. Elsberry, 2017: Ending storm version of the 7-day weighted analog intensity prediction technique for western North Pacific tropical cyclones. *Wea. Forecasting*, **32**, 2229-2235.

Velden, C. S., D. C. Herndon, J. P. Kossin, J. D. Hawkins and M. DeMaria, 2006: Consensus estimates of tropical cyclone intensity using integrated multispectral (IR and MW) satellite observations. *Preprints, 27th Conference on Hurricanes and Tropical Meteorology*, Monterey, CA, Amer. Meteor. Soc.

Wang, C., and Z. Zeng, 2018: Influence of model horizontal resolution on the intensity and structure of Rammasun. *J. Trop. Met*, in press.

Wood, K. M., and E. A. Ritchie, 2015: A definition for rapid weakening in the North Atlantic and eastern North Pacific. *Geophys. Res. Lett.*, **42**, 10091-10097.

Wu, C.-C., T.-H. Li, and Y.-H. Huang, 2015: Influence of mesoscale topography on tropical cyclone tracks: Further examination of the channeling effect. *J. Atmos. Sci.*, **72**, 3032-3050.

Xu, J., and Y. Wang, 2015: A statistical analysis on the dependence of tropical cyclone intensification rate on the storm intensity and size in the North Atlantic. *Wea. Forecasting*, **30**, 692–701.

Yu, Z., Y. Wang, H. Xu, N. E. Davidson, Y. Chen, Y. Chen, and H. Yu, 2017: On the relationship between intensity and rainfall distribution in tropical cyclones making landfall over China. *J. Appl. Meteor. Climatol.*, **56**, 2883–2901.

Zeng, Z.-H., Y. Wang, and C.-C. Wu, 2007: Environmental dynamical control of tropical cyclone intensity: An observational study. *Mon. Wea. Rev.*, **135**, 38–59.

Zhang, F., Z. Pu, and C. Wang, 2017: Effects of boundary layer vertical mixing on the evolution of hurricanes over land. *Mon. Wea. Rev.,* **145,** 2343-2361.